FABRICATION AND TESTING OF BIOMIMETIC MICROSTRUCTURES FOR WALKWAY TRIBOMETERS

Christopher W. Haney

Thesis Prepared for the Degree of

MASTER OF SCIENCE

UNIVERSITY OF NORTH TEXAS

December 2019

APPROVED:

Hector R. Siller, Major Professor
Huseyin Bostanci, Committee Member
Seifollah Nasrazadani, Committee Member
and Interim Chair of the Department
of Engineering Technology
Hanchen Huang, Dean of the College of
Engineering
Victor Prybutok, Dean of the Toulouse
Graduate School

Haney, Christopher W. *Fabrication and Testing of Biomimetic Microstructures for Walkway Tribometers*. Master of Science (Engineering Technology), December 2019, 108 pp., 16 tables, 55 figures, 1 appendix, 19 numbered references.

The main objective of this work is to give contribution in both additive manufacturing (AM) and tribometry derived from the application and study of materials available with the use of biomimetic designs. Additional contributions are determining what effects treatments for flooring surfaces may have on the dynamic coefficient of friction and the effects of these products on common surfaces. The validity of the proposed methodology for a proof of concept was demonstrated by comparing measured dynamic coefficient of friction for designs using standardized equipment and comparing these values to plantar skin tested using an accepted and standardized testing method that has been extensively researched and validated. Initial biomimetic designs and characteristics unique to each design were researched and compared. Eleven designs were selected to be fabricated, tested, and compared to select the most desirable applications for further investigation. Research into potential treatments commercially available for use was done to determine the efficacy of these products. Prototype sensor designs were selected and fabricated using direct light processing (DLP) technology. Examination of the measured values was done through an analysis of the variances in the response variable and comparisons using Fisher and Tukey pairwise comparison method. Future work recommendations are provided for further development and improvement of the topics presented in this thesis.

ACKNOWLEDGEMENTS

I would like to voice my sincere and immense gratitude to my advisor Dr. Hector R. Siller for his excellent technical proficiency, endless guidance, and remarkable support. It has been a pleasure to be your graduate research assistant and your student. Thank you Dr. Siller, the skill and knowledge gained from working with you has educated me more than any credit I can give.

I would like to extend my gratitude to Dr. Huseyin Bostanci and Dr. Seifollah Nasrazadani for being part of my thesis committee and for providing significant feedback and recommendations to effectively improve the quality of the work presented in this thesis.

I am thankful to Erick Ramirez-Cedillo who has played a role during the development of this thesis. Erick was always pleased to share his expertise in additive manufacturing. In addition, I take this chance to express gratitude to my research colleagues, the Engineering Technology Department, Regan Scientific Instruments and Walkway management group, and all my friends for their meaningful support.

Most notably, none of my accomplishments could have happened without my family. To my older brothers and sisters: Chad Haney, Derek Haney, Charles Haney, Elizabeth Thrailkill, and Carrie Cody, whose guidance and support have aided me in my journey. I would also like to express my gratitude to my nieces and nephews for always being a continuous and contagious positive influence on my life. Thank you for all the valuable memories and always believing in my ability to be successful in the academic field. Thank you, mom and dad, for your unconditional love and your extraordinary help. All of this could not have happened without everyone’s support.

TABLE OF CONTENTS

LIST OF TABLES

Page

LIST OF FIGURES

CHAPTER 1

INTRODUCTION

1.1 Background and Motivation

Research and growth of additive manufacturing processes has increased in the last decade. The ability to rapidly produce prototypes, reduce weight, and maintain certain mechanical properties with limited resources is an immense benefit of 3D printing. The ability to print certain designs that other traditional manufacturing processes would be incapable or otherwise very costly to do, can be done quite easily through resources of additive manufacturing. The liberty allowed by these manufacturing processes stimulates the demand of these processes in many sectors of the economy.

While many of the practical applications of additive manufacturing are focused in the biomedical field, aeronautics, topology optimization, and academics a significant lack of research into the application for tribometry and biomimetics is present. Practical applications of 3D printing in regards to tribological applications is scarce while benefits are present such as decreasing friction in fluid systems and improving frictional properties in necessary structures. Many insects, plants, reptiles, and animals have adapted and formed structures to aide them in their respective environments. Butterflies have evolved to form sharp ribs on their bodies and lotus leaves have developed small circular structures to promote super-hydrophobicity and dry adhesion. Sharks skin consists of complex repeating patterns that help to promote anti-fouling while reducing drag experienced underwater. Lastly gecko’s have developed long spatula like structures to increase their ability to adhere to dry surfaces, and moth-eyes have developed small round bumps in a fixed pattern to help increase friction reduction and anti-reflection properties [1]. Over several thousand years these traits have become more prominent in these species in order to achieve a specific goal necessary for survival. These biomimetic surfaces can be applied in order to achieve desired results. Such benefits could be the increase of friction in a system to better improve an already existing product. Alexey Tsipenyuk et al. applied hexagonal patterns to razor guards in order to facilitate excess fluid drainage from the contact area which yielded better results than the commercially available razor products [1]. They found that properly designed hexagonal structures could increase the available friction of the lubricated skin by almost twice as much as the standard razor blade. Ajay Malshe et al. found several designs that could be applicable in self-adhering patches using designs based on a gecko's dry adhering abilities [2]. These experiments have detailed the practical applications of biomimetic designs in everyday applications.

These biomimetic structures will be selected on their potential applications, drafted, then fabricated using traditional or non-traditional manufacturing means. These designs will then be tested under controlled experimental conditions. Samples will be designed and initially fabricated using DLP printing to determine feasibility. These designs will be tested under a controlled design of the experiment. This will also serve to determine the possibility to replicate designs in a high production environment with a high degree of repeatability and reproducibility. Some designs have already been applied and tested in some experiments to achieve desired properties such as an increase the available friction, reducing drag, and increasing the hydrophobicity of a design. The broad range in available resins to be used in direct light printers is a large benefit of this process. Additive manufacturing provides much more freedom in designing than what is available through traditional processes such as computer numerical controllers (CNC) and electrical discharge machining (EDM). Once a digital model is created the design can be fabricated by printing layer-by-layer until the sample is finished. AM provides the ability to create more complex designs, faster merchandise development processes, less interaction due to humans reducing potential variation, and a reduction in costs because of the ability to produce goods consistent about a nominal value. Therefore, AM has a vast potential in successfully realizing the application of biomimetics for everyday applications. It is optimistic that through this research into biomimetic designs combined with AM and tribometry that a significant contribution can be made in improving pedestrian walkway safety across the board by properly assessing the surfaces in regards to plantar skin dynamic coefficient of friction (DCOF) performance.

1.2 Problem Statement

Integration of biomimetics and additive manufacturing is a tremendously rewarding process, starting a growing relationship, where new pioneering ideas can be realized with additive manufacturing. However, AM is not without limitations and understanding these is just as important as understanding its capabilities, and integrating them during the design process will lead toward many beneficial results. Stated earlier, the application of biomimetics in AM is scarce. Notwithstanding the exceptional evolution of additive manufacturing over the last three decades, the development of engineering designs to take advantage of the possibilities offered through additive manufacturing and to mitigate the constraints related with the technology has significantly lagged behind the fabrication of different AM processes.

1.3 Thesis Scope, Goals and Objectives

The purpose of this thesis is to give a modest contribution in filling the gap between design and additive manufacturing by applying biomimetics. The proposed methodology is applied in a real-world scenario. The application of biomimetic designs in AM adjoined with proper material selection to reproduce mechanical properties associated with human skin is the focus of this thesis. The objectives of this thesis are to:

- Research biomimetic designs and the possible applications of each design and the impact they may or may not have on the frictional measurements while using a walkway tribometer.
- Develop a methodology for design, customization, fabrication, and validation of obtained measurements in regards to human skin. Demonstrate the validity of the proposed experimental methodology by comparing it to accepted measurement standards.
- Design, validate, and select the proper biomimetic structure for plantar skin substitution in measurements and improve walkway safety.
- Fabricate testing samples and final models using additive manufacturing technologies.
- Validate the generated results and to propose further improvement ideas.

1.4 Definitions and Abbreviations

- μ - used in equations to represent the value for the coefficient of friction also used to represent micrometers
- AM – Additive manufacturing
- ANOVA – analysis of variance

- ANSI – refers to the U.S. private non-profit association that oversees standards for manufactured goods, services, procedures, methods, and personnel.
- ASTM – refers to the international standards association for testing and materials.
- BOT – Binary output tribometer, used to refer to the BOT3000E a drag sled measurement device.
- BST – used to refer to the BST 2000, a drag sled measurement device
- cm/s – centimeters per second, used to account for the speed of the equipment.
- CNC – Computer numerical control, used to refer to automated control of tools for machining.
- COF – acronym used to represent the coefficient of friction.
- DCOF – Dynamic coefficient of friction.
- DIN – Deutsches Institut fur Norming, German counter-part to ANSI
- EDM – Electrical discharge machining, used to refer to a nontraditional form of manufacturing utilizing electricity and conductive material to remove the material.
- GMG – used to refer to the GMG-200 a drag sled measurement device.
- N – Unit for Newtons for forces, also used to represent the normal force in calculating the DCOF.
- n – Used to represent the number of samples in the coefficient of correlation value tables.
- Pend – an abbreviated form of pendulum, used to refer to the pendulum method for measuring the DCOF
- Rxy – used to represent the coefficient of correlation value.
- SAE – Society of Automotive Engineers
- SBR – styrene-butadiene rubber relates to the BOT3000E as the standardized rubber used to measure the DCOF.

- SLS – This abbreviation refers to sodium lauryl sulfate, used as a wetting agent for some standards associated with certain equipment and is an anionic detergent and surfactant.
- STF – acronym used to represent slips, trips, and falls.
- TCNA – Tile Council of North America

1.5 Organization of the Thesis

The organization of this thesis is as follows. Chapter 1 discusses the overall presentation of the proposed work by explaining motivations, problem identification, scope, goals, objectives, relevant definitions, and the structure of the thesis. Chapter 2 provides a background on the accepted frictional measurement methods, a fundamental concept review of accepted frictional measurements, and methods or technologies upon which this thesis is built. Chapter 3 is focused on the main area of the thesis which is the selected AM process and measurement equipment, the design for the experiment establishing the desired methodology for testing, and obtained results for the treatment study and the application of the biomimetic designs on a walkway tribometer. Chapter 4 covers the statistical analysis of the obtained values from the experiment. Finally, chapter 5 consists of conclusions of all the work presented and suggestions for further improvements and future research applications. Prototype designs and images of the DLP samples will be provided.

CHAPTER 2

LITERATURE REVIEW

2.1 Accepted Friction Measurement Methods

In the following section the different accepted methods for measuring the coefficient of friction on a surface are discussed along with pros and cons of each method. The procedure, history, and relevant standards for each method is also included and referenced. The associated fundamental methods for each method is discussed as well within chapter 2. The accepted methods are as follows:

- DIN 51130 & Variable Angle Ramp[3]
- British Pendulum Method
- SlipAlert Slip Resistance
- ANSI A326.3 & BOT-3000E [4]

Additionally, in this section factors that can impact the measured DCOF while walking is discussed. This section also covers the literature review where influencing papers that provided the foundation for this thesis are discussed and covered. Finally, a table correlating the different methods together is provided.

2.1.1 DIN 51130 Variable Angle Ramp

The variable-angle ramp system was established and made in Germany between the cooperation of the German government, and the University of Wuppertal. The method is commonly referred to as the “German ramp method.” This method is considered to be a standard for comparisons between methods for measurement of DCOF and slip resistance of surfaces. The method calls for the use of a safety harness and subjects walking across a surface while the angle of incline is increased. This specific process has been used to take measurements of surfaces in laboratories for almost a quarter of a century. After the method was created, additional research was conducted by Dr. Stefan Bönig at the University of Wuppertal in determining a standardized limit for the coefficient of friction needed for slip resistance while walking[5].

The method for using the DIN 51130 is simple and straightforward to use. This event is carried out by two researchers, one who walks across the surface and another who slowly increases the incline until a slip occurs. Samples of surfaces are mounted onto the variable-angle ramp and the tester is harnessed to a safety line to prevent injuries. The test can be carried out in a standardized boot or barefoot (Figure 2-1). The tester then walks up and down the flooring sample taking small steps while gradually increasing the incline until the operative slips. The rate of increase for the angle should be approximately 1°/sec. The slant of the inclination is then recorded once a slip occurs and the test is repeated an additional two times for a total of three angle measurements. An average from these three angles is then calculated, then the tangent of that angle is taken to reach the DCOF value [6].

This method has been repeatedly tested and the results confirmed. Not only does the method have significant repeatability, but it can also perform tests in dry or wet conditions with or without footwear. The most prominent benefit of this method is due to the fact it measures human ambulation across a specific surface. The largest problems for this method are attributed to the size of the ramp. This event limits its portability and confines its use to laboratories and laboratory samples. This issue means that a specific sample at a given location cannot be tested without having to endure large expenses to remove the sample from the location and transport it for testing. However, this method still holds merit with its limited use and provides a baseline for comparison of other methods to be made [3].

Figure 2-1: Variable angle ramp

2.1.2 SlipAlert Slip Resistance

SlipAlert is a new British Standard slip test used to measure the slipperiness of a surface. The design of the SlipAlert is meant to be more portable and accurate across all surfaces. The method SlipAlert is fundamentally the same as the pendulum method and correlates well to one another. Both of these methods are accepted British methods for measuring the slipperiness of a surface. The concept for this method is to deliver consistent potential energy to the test surface. The SlipAlert cart is elevated up on a ramp to obtain a consistent and proportional amount of energy. The slip cart uses a rubber test foot mounted at a specific angle. As the cart travels down the ramp, the ramp allows the slider to not come into contact with the surface until all of the front axle is traversing the test surface. Once the slider begins to come into contact with the test surface, the wheels of the cart are lifted and disengaged. The distance traversed by the cart is then determined by the frictional force between the slider and the sample surface. This distance is recorded by a counter fixed to the cart powered by a 9V battery that can be reset for each use. A scale has been developed to determine the relative slip resistance measured by the distance covered by the front wheels. Each test surface has a specific testing foot to be used and can simply be changed out by removing a bolt. If the value obtained from the test falls under 130 SlipAlert Test Value (STV), the floor is considered to be safe. Should the surface range from 130+ to 173, it is considered to be a medium risk of slip and manageable, should the value be higher than 173, the risk for a slip is considered to be high.

The benefits of this testing method are that the method is simple, portable, and quick to use. This method was developed to be used on a variety of surfaces and surface conditions. It can be used on slopes to measure slip resistance unlike other methods and additional procedures have been made to compensate for the additional potential energy. Additionally, there are little technical features of the cart and hence requires bare minimum maintenance of the equipment such as resetting the counter and changing the 9V battery. Users can easily read the output of a single value variable making the cart simple to use. Drawbacks to this method are that it does not directly measure DCOF or SCOF, instead measures energy loss between the contact surface and flooring surface then converted into friction values. The rolling distance merely suggests the magnitude of available friction in that specific direction. This method has not yet had the opportunity to undergo as much testing as other methods, but it does correlate efficiently to the sister method of the pendulum [7].

2.1.3 British Pendulum

The British pendulum was originally developed and designed in the 1940s in the United States and then further developed and researched in the United Kingdom Transport Research Laboratory during the 1960s to be used in testing road surface conditions. It was designed for both labs and on-site testing. Additionally, the method is accredited under ISO 9001:2000 and established as an ASTM standard (ASTM E 303) and validated in 1971 by testing results on walking surfaces obtained for more than twenty-five years. It also received the highest correlation with human traction in a peer-reviewed study published a scientific study of eleven types of tribometers by the University of Southern California Medical Center. The pendulum method has been widely adopted and has situation-specific standards established in the HB198 of Standards Australia. The method has been adopted and is used in over fifty nations for the assessment of pedestrian walkway safety.

As discussed in the previous section, the British pendulum method is an accepted standard for determining the slip resistance of a surface and is an accepted measurement method for pedestrian slip resistance. The pendulum (Figure 2-2) uses a standardized type 96 rubber fixed to the foot of the pendulum which is set to travel a fixed distance across the surface via adjustments made to the height of the pendulum. The travel distance is set to roughly 123-125mm. Before tests are carried out at that specific distance, the pendulum should be fully leveled, then the pendulum height should be raised so that it can swing freely without resistance. The arm should be raised into its locking position and released. The pointer on the face of the tester should read zero before any tests are conducted. Should it not read zero, adjustments to the pointer mount should be made by adjusting the O-ring to increase or decrease the amount of friction between the pointer and the pendulum. This process should be repeated until the results consistently reach a zero reading. After this event has been done, adjust the pendulum to lower the sliding foot so that it will traverse a distance between 123-125mm. Tests can be conducted in wet/contaminated conditions or dry. Raise the pendulum arm into the locking position, then press the release to allow the arm to swing and slide across the surface. The arm will need to be caught after the full swing has been made, so that it does not move the scale pointer and affect the results of the test. The results should be recorded and the test should be carried out multiple times to determine the state of the surface in question.

Figure 2-2: Knightcott Surface Solutions Pendulum

Benefits of this method are that it has been repeatedly tested and validated. Additionally, it is widely accepted across the globe and has international acceptance in courts of law. It is relatively easy to use with appropriate training and understanding of the principles at use. The pendulum operates on the use of potential energy from being raised to a fixed height to measure the slip resistance of a surface as the slider traverses the surface (Figure 2-2). The drawbacks of this method are that the pendulum can be difficult to carry out in the field. Additionally, time is required before each testing is conducted to ensure the system is properly calibrated so users receive an accurate reading. With practice, setting the traveling distance and preparing the slider can become relatively easier, but still requires adequate preparations. A scale has been developed that converts the pendulum test values into a coefficient of friction. The scale does not measure upwards of 1.0 [8][9].

2.1.4 BOT3000E

Regan Scientific Instruments, Binary Output Tribometer (BOT) has the ability of doing both static and dynamic coefficient of friction measurements. The BOT-3000E like the pendulum method passed the ASTM F2508-13, a standard for the validation, calibration, and certification of walkway tribometers using a reference surface (Figure 2-3 and 2-4). The BOT-3000E also has ANSI test methods specified for its use in the measurements of DCOF for level interior surfaces such as A326.3[4] which has been mentioned before. The concept behind the BOT-3000E is the same as other drag sleds in that the machine propels itself across the surface using at a constant speed of 20cm/s ± 5% measuring the resistance of the surface to the normal force of 22.4N ± 2% of the SBR rubber insert that is loaded to the bottom. This fact means there is little human input into the results of the test besides the pushing of a button to begin the test. As the SBR insert traverses the surface set to a user-defined distance between four inches up to thirty-six inches, a strain is applied to a gauge inside that measures the amount of force being produced. These tests can be conducted in both wet and dry conditions. However, in wet conditions, enough of the fluid should be applied that the SBR sensor will remain in the fluid during the entirety of the tests.

Figure 2-3: BOT3000E drag sled side view

Figure 2-4: BOT3000E drag sled top view

Before using the BOT-3000E proper steps should be taken to ensure that it is in calibration. This process begins by inserting a provided verification mass that is specific to each BOT. Once the verification mass process has been conducted and passes the next step is to ensure the SBR sensor is properly prepared. An examination of the SBR insert should be conducted before, during, and after each test to evaluate wear. Should a prominent wear line be present on the sensor, reconditioning should be done. The sensor should be inserted into the reconditioning tool until a uniform surface free from defects is produced. The surface should then be brushed to ensure no additional debris may be present. Next, the provided reference surface should be cleaned using an approved surface cleaner. The SBR sensor should then be placed into the bottom of the BOT-3000E and 0.05% SLS solution should then be applied evenly across the reference surface to ensure the SBR sensor will remain in the surfactant during the test. A single test run should be done across the reference surface in one direction, then rotate 180° back across the surface. The two DCOF measurements should then be averaged and should fall near 0.40 ± 0.03. Once this process has been completed, and the BOT-3000E passes, testing can be conducted where the DCOF value will be displayed on the LCD TFT screen.

Benefits of using the BOT-3000E are that there is little human interaction that could affect the results. The BOT-3000E also records images of the surface during testing, conducts 1000 samples/sec, and generates viewable graphs from measurements automatically. The BOT-3000E is capable of taking measurements for DCOF ranging from 0.01 to 1.00 and is lightweight and portable. Thousands of measurements can be recorded and stored to the BOT's memory and retrieved via a USB drive and possesses the ability of printing out the results from each test including the measured DCOF value, temperature, humidity, and the conditions applied and selected by the user for each test. It is also accepted to be used in court cases in both the United States and Canada and can help to remove potential slipping and falling hazards to be following the Standard of Care in OSHA Section 5(a)(1), general duty clause. Additional programs are provided by Regan Scientific Instruments in the proper use of the BOT-3000E to become an official auditor. Finally, Dr. Jens Sebald of the University of Wuppertal located in Germany tested the BOT-3000E measured DCOF against the adhesive friction of people walking across seventy-two test points that included twelve surfaces, two different emollients, and three separate materials used on shoes. A coefficient of correlation of 0.93 was obtained. Drawbacks to the use of the BOT are the BOT being unable to progress across rough or smooth surfaces, however, this event can be easily mitigated by providing suitable traction for the BOT. Preparation time is moderate but vital to ensure the results obtained are valid and indicative of the surface conditions. Due to the high sampling rate, accuracy, repeatability, and correlation, the BOT-3000E was selected to be used to evaluate the effects of microstructures on the dynamic coefficient of friction[10]

2.1.5 Coefficient of Correlation

Correlation coefficients are used in statistics to measure how strong the relationship is between different sets of variables. A value near 1.0 represents a strong agreeable relationship between the samples. In the tables created by Dr. Jens Sebald, variable *rxy* represents the correlation coefficient for the given equipment. Variable *n* is the number of data points related to the particular section of the table for comparison. BST, GMG, and BOT are all variations of the drag sled principle, *pend* is the pendulum method, and *ramp* represents the variable-angle ramp method. Table 2-1 shows the coefficients of correlation between the accepted methods for measuring the dynamic coefficient of friction using SAE 10W-30 motor oil and Table 2-2 shows the correlations using water+SLS at a 0.05% solution. These values are measured for the three types of sliders used on twelve separate floor coverings. Note the correlation between the methods. Using SAE 10W-30 motor oil the correlation values between the accepted ramp method and the BOT3000E is 0.989 using SBR and averages 0.964 across the thirty-six samples. The BOT also correlates 0.947 to the pendulum method using SBR and averages 0.837 across the thirty-six samples. Correlation values below 0.70 are considered to be poor correlations and are grayed in the tables.

Table 2-1:Coefficients of correlation with SAE 10W-30 SAE oil lubricant[11]

		Slider/shoe S20 (SBR)				Slider/shoe S25 (Picasso)			
		BST (position 0°)	GMG	BOT	Pend	BST (position 0°)	GMG	BOT	Pend
Ramp (μ=tanα)	(rxy)	0.985	0.966	0.989	0.927	0.989	0.949	0.962	
	(n)	12	12	12	12	12	12	12	
BST (position 0°)	(rxy)		0.987	0.99	0.942		0.956	0.966	
	(n)		12	12	12		12	12	
GMG	(rxy)			0.988	0.956			0.948	
	(n)			12	12			12	
BOT	(rxy)				0.947				
	(n)				12				
		Slider/shoe S04 (H range)				All 3 Sliders			
		BST (position 0°)	GMG	BOT	Pend	BST (position 0°)	GMG	BOT	Pend
Ramp (μ=tanα)	(rxy)	0.944	0.896	0.955	0.799	0.968	0.941	0.964	0.768
	(n)	12	12	12	12	36	36	36	24
BST (position 0°)	(rxy)		0.954	0.98	0.932		0.944	0.96	0.893
	(n)		12	12	12		36	36	24
GMG	(rxy)			0.967	0.912			0.971	0.834
	(n)			12	12			36	24
BOT	(rxy)				0.9				0.837
	(n)				12				24

Table 2-2: Coefficient of Correlation with water-SLS mixture at 0.05% solution [11]

		Slider/shoe S20 (SBR)				Slider/shoe S25 (Picasso)			
		BST (position 0°)	GMG	BOT	Pend	BST (position 0°)	GMG	BOT	Pend
Ramp (μ=tanα)	(rxy)	0.817	0.893	0.879	0.687	0.765	0.584	0.695	
	(n)	12	12	12	12	12	12	12	
BST (position 0°)	(rxy)		0.892	0.788	0.738		0.843	0.809	
	(n)		12	12	12		12	12	
GMG	(rxy)			0.926	0.618			0.884	
	(n)			12	12			12	
BOT	(rxy)				0.614				
	(n)				12				
		Slider/shoe S04 (H range)				All 3 Sliders			
		BST	GMG	BOT	Pend	BST	GMG	BOT	Pend
Ramp (μ=tanα)	(rxy)	0.894	0.826	0.857	0.651	0.823	0.788	0.812	0.686
	(n)	12	12	12	12	36	36	36	24
BST	(rxy)		0.871	0.928	0.822		0.865	0.863	0.803
	(n)		12	12	12		36	36	24
GMG	(rxy)			0.844	0.635			0.887	0.65
	(n)			12	12			36	24
BOT	(rxy)				0.812				0.748
	(n)				12				24

The BST and GMG are both drag sleds which employ the same principle but operate under different conditions. The BST is based on the same design as the FSC2000 pictured below. The largest difference between the BST, FSC, and BOT is due to the strain gauges utilized in the equipment for the measurement of the DCOF and their testing parameters. The GMG uses three separate flat sliders versus the BST, FSC, and BOT which utilize only a single curved slider with a radius of 0.68mm. Images of these sliders and equipment can be seen in Figure 2-5.

These correlation values and information are important as they help in setting up an experiment which will yield reliable results between the methods. Since testing has already been done showing that the best correlation between the variable angle ramp and the BOT3000E drag sled is with 10W-30 SAE oil, this will be the initial lubricant used at this time. Furthermore, since the slider sensor utilized is curved; only a small portion of the sensor actually comes into contact with the surface. A full design covering the entire sensor is not entirely necessary aside from aesthetics for the assessment of the flooring. This means that a full sensor design is not required for testing, but sufficient material should be present to ensure that the entirety of the contact section of the sensor is covered for accurate measurements

Figure 2-5: FSC and GMG drag sled and slider images [12]

2.2 Fundamentals of Friction Measurement Review

In this section the fundamental and free-body diagrams for each of the three measurement principals: drag sled, pendulum, and variable angle ramp is discussed. The equations and calculations for acquiring the COF for each of the methods is provided as well.

2.2.1 Drag Sled – Frictional Force

The drag sled method for measuring the dynamic coefficient of friction functions by measuring the ratio of the frictional force, and the normal force as the sled moves across the surface. The frictional force will always be the opposite of the direction of travel. The magnitude of the force is highly dependent on the interaction of the two materials and the lubricating medium. The measured value is dimensionless and scalar

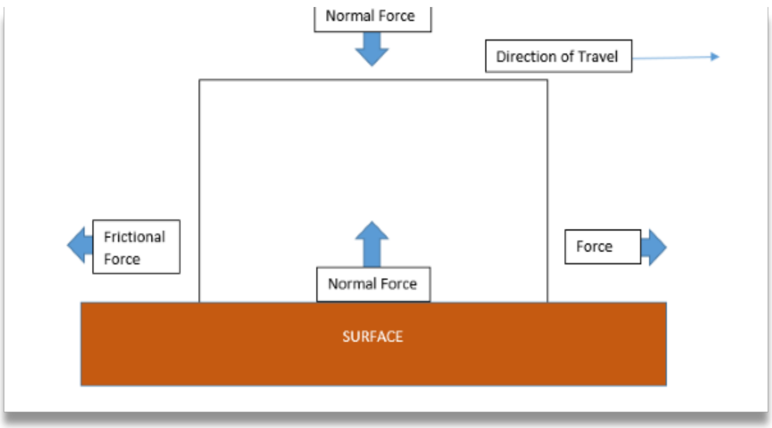

(Fig. 2-6).

Figure 2-6: Drag Sled Free Body Diagram

The diagram models the behavior and factors that occur during the proposed method. The normal force is determined either by the weight of the sled or has a controlled normal force that remains constant throughout the testing. The interaction between the two surfaces is highly dependent on their ability to form adhesive bonds during the slow-moving speeds[13][5]. The relevant equation for determining the coefficient of friction using the drag sled method is:

$$\mu = \mathrm{Fr} \div \mathrm{Fn} \qquad \text{[Eq. 2-1]}$$

2.2.2 Pendulum – Frictional Energy Loss

The Pendulum and SlipAlert method for the measurement of the dynamic coefficient of friction operates by measuring the amount of energy lost due to friction to determine the DCOF. The equation subtracts the final work from the initial work done in potential energy due to gravity moving along a circular path divided by the normal force of the equipment in use multiplied by the skidding distance to determine the dynamic coefficient of friction. On both of these devices a scale has been developed to convert

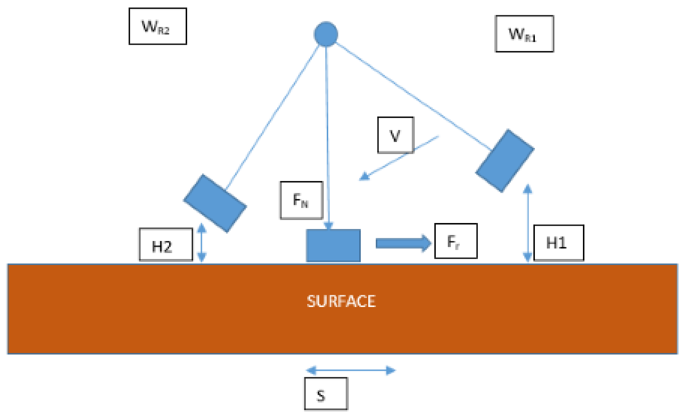

what is known as PTV (pendulum test value) to a DCOF value. Figure 2-7 models the principle behavior that occurs during both SlipAlert and the pendulum method[5].

Figure 2-7: Pendulum Free Body Diagram

The measured value is then determined through energy loss during testing due to frictional forces that occur during the fixed skidding distance for the pendulum and the distance travelled by the SlipAlert. The equation to model this behavior is:

$$\mu = \frac{(W_{R1} - W_{R2})}{(F_N * s)} \qquad \text{[Eq. 2-2]}$$

2.2.3 Variable Angle Ramp: Slip Angle

The DIN 51130 variable-angle ramp method for the measurement of the dynamic coefficient of friction operates by measuring the critical slip angle of a surface. The equation for the measurement takes the tangent of the angle the ramps make at the time a slip occurs. During walking the force generated – *F* can be divided into a horizontal force – *R* and vertical force – *T* along the surface. The vertical force is always

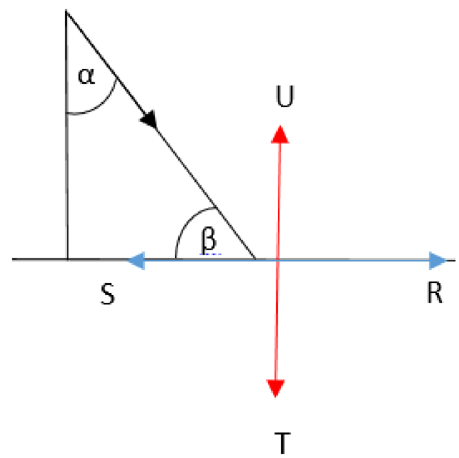

exactly balanced by the reaction force – *U*, however, at times the horizontal force can exceed the resisting frictional force – *S* causing a slip to occur. For no-slip to occur, all forces must be equally balanced and in equilibrium (Figure 2-8).

Figure 2-8: Heel-strike resolution on level surface

$$T = U \qquad \text{[Eq. 2-3]}$$

$$R = S \qquad \text{[Eq. 2-4]}$$

So, the max frictional force available is the coefficient of friction – μ multiplied by the normal force – *U*,

$$S = \mu U \qquad \text{[Eq. 2-5]}$$

then

$$\mu = \frac{S}{U} \qquad \text{[Eq. 2-6]}$$

If the angle the leg makes with the vertical can be taken as α, then the maximum frictional force would be:

$$S = Fsin(\alpha) \quad \text{[Eq. 2-7]}$$

The resolution for the vertical force would be:

$$U = Fcos(\alpha) \quad \text{[Eq. 2-8]}$$

With the relation between the horizontal and vertical forces known, the equation for the coefficient of friction would resolve to:

$$\mu = \tan(\alpha) \quad \text{[Eq. 2-9]}$$

where a step can be defined as $2Lsin(\alpha)$where *L* is the length from the hip to the heel of the foot. The angle β the leg makes with the horizontal can then be defined as $\mu = \cot(\beta)$ and is the critical angle that occurs during a slip (Figure 2-9). Should a shorter step be taken the angle α would, therefore, be smaller, the vertical force *T* would be larger, and the horizontal force *R* would be smaller. In this scenario, enough frictional forces would then be provided to balance *R*.

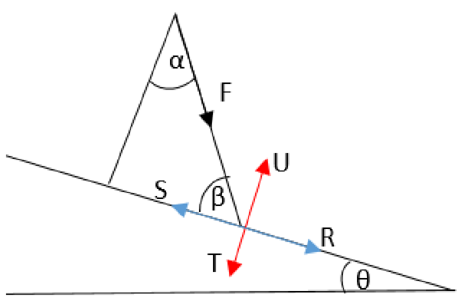

Figure 2-9: Heel strike force resolutions on a sloped surface

If the surface present in Figure 2-9 were to be tilted through an angle *θ*, the same analysis can be used to resolve the forces (Figure 2-10).

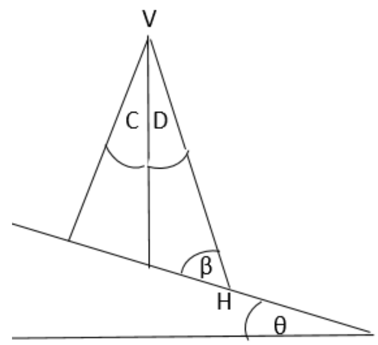

Figure 2-10: Upright body position on a sloped surface

The downward force *F* can be resolved into two components: one perpendicular to the surface, and one along the surface. The equation $\mu = Cot(\beta)$ is obtained. For a person to maintain balance while walking down an inclined surface, a person must remain upright. Angle *α* can be split into two angles *C* and *D* and the equation $\mu = \tan(\alpha)$ becomes$\mu = \tan(C + D)$.

Arithmetically, this is the same as $\mu = \tan(\alpha)$ but represents a different step length since angle *D* is smaller than angle *α,* and the length of step is$2Lsin(D) * \sec(C)$. Thus, on a sloped surface, the critical angle *β* is reached at a shorter step versus walking on a level surface. As the angle θ increases, shorter steps must be taken to maintain balance until *VH* becomes vertical and *D* becomes zero and $\mu = \tan(C)$. After this point is reached, no step can be taken without a slip occurring since *C* is equal to *θ* then $\mu = \tan(\theta)$. It is then at this point where the angle D becomes zero and the COF is directly related to the tangent of the slope [5][6].

2.2.4 Factors in DCOF

The following sections will cover the analytical factors and the factors that can affect the measurable DCOF values. It is important to note that walking is a highly dynamic process with constant shifts in balance and corrections being made.

2.2.4.1 Analytical

The mathematical formula for calculating the coefficient of kinetic friction otherwise named the dynamic coefficient of friction is given by the following formula:

$$\mu_k = \frac{F}{N} \qquad \text{[Eq. 2-10]}$$

μ = Coefficient of kinetic friction or static friction

F = Force of kinetic friction in Newtons

N = Normal force in Newtons

The force of dynamic friction that is experienced between two interacting surfaces traversing one another acts against the movement. The magnitude of this force is highly dependent on the interaction of the two materials. This event leads to a specific coefficient of friction for the interaction between both different materials and mediums. The coefficient of friction has no units and is dimensionless. DCOF and SCOF are scalar and hence the direction of the force has no effect on the objective quantity. Note that previously an accepted measurement for measuring the slip resistance of a surface was through the measurement of the static coefficient of friction. This event has recently been rejected and more focus towards the measurement of slip resistance for a surface through the measurement of the dynamic coefficient of friction. A free-body diagram of the interactions that occur is represented below (Figure 2-11).

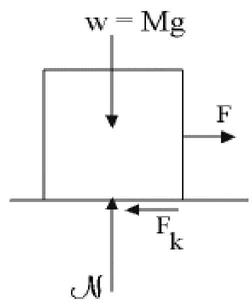

Figure 2-11: DCOF free body diagram

Static friction can be defined as the amount of force necessary for an object to remain stationary while a force acts on the object. Static friction is present until the object begins moving. If the amount of force applied to an object is equal to the static friction of the surface then the object is close to slipping. For the object to continue moving the externally applied force shall be greater than the force of static friction. For the dynamic coefficient of friction, objects are already in motion. Should the force that is externally applied be equal to the force of dynamic friction then the object will move across the surface at a constant velocity. Because of this relationship $\mu_s > \mu_k$. Due to the lack of time to form bonds. This process, however, becomes much more complicated when applied to a simple process such as walking [5].

2.2.4.2 Walking Factors

Walking is a highly dynamic process. There are several potential factors that can lead to a slip or fall scenario (Figure 2-12). Throughout an entire gait cycle, a person spends about twenty percent of the time with both feet on the ground in a stance of double support. This amount of time, however, decreases as velocity increases. During sprinting there exists points in time where both feet are off the ground. For the purpose of this thesis, the focus will remain around walking. Walking can be broken down into two phases: stance and swing. The stance phase accounts for roughly sixty percent of the entire walking process and about forty percent for the swing phase[14]. The stance phase begins with a heel contact followed by flat foot contact, and then a push-off or heel off. The stance phase then begins with a swinging of the leg and ends with a heel contact. Gaits can vary from person to person and be heavily affected by not only the age and gender of the person but also by diseases, injuries, loss of balance, and the type of shoes worn. These details are critical in the understanding of the coefficient of friction because of the impact they have on the potential for an accident to occur, and the ability to assess the safety factor of a surface. In a study conducted on the effect of footwear on the measured values of balance and gait in women between the ages of sixty-five and ninety-three years old, it was found that subjects performed better when they wore regular walking shoes or the subjects were barefoot[15]. Because of this, it is important to note that adhesion is one of the most influential factors in dry rubber friction at low speeds[13].

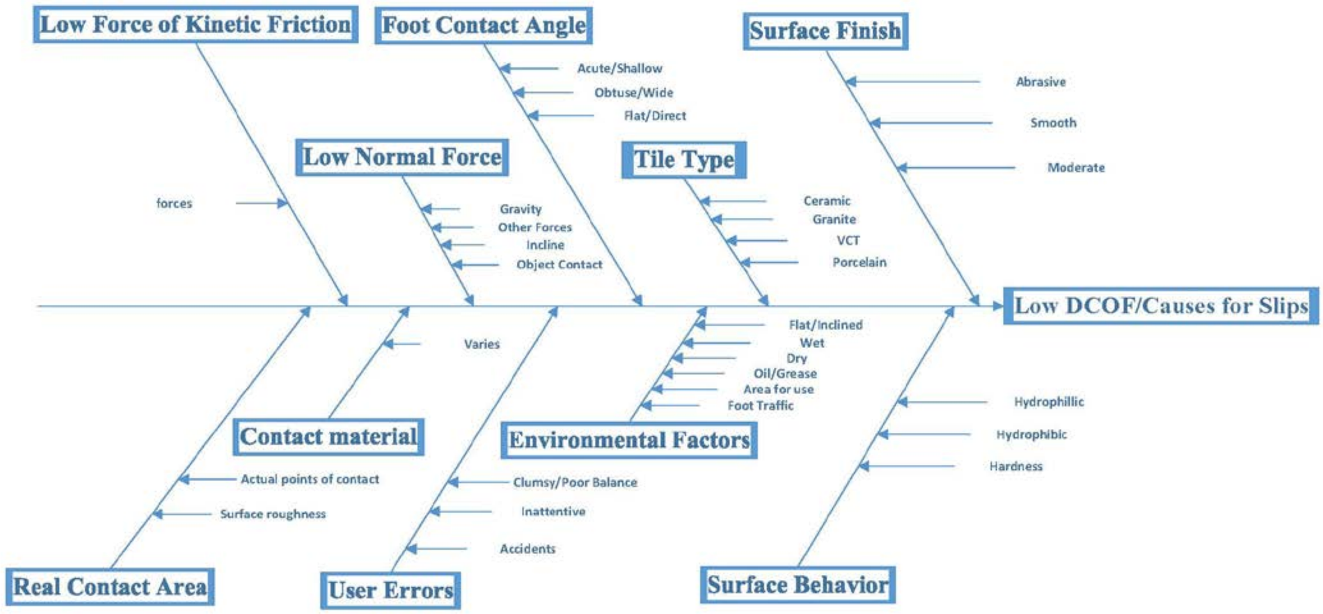

Figure 2-12: Cause effect diagram for contributing factors to slips, trips, and falls

The simple calculation for the kinetic coefficient of friction now becomes much more complicated when considered into a process such as walking. Several additional factors have been modeled in the following diagram for consideration into potential causes that may attribute to a slip and fall. Any factor that can lead to an increase in the normal force that is experienced can lead to a large decrease in the coefficient of friction. This issue could be caused by micro-adjustments by a person during walking, increase in velocity, shoe material, and premature shift in weight distributions during transitional phases of walking. These are just a few of many factors that may be present. Additional factors that can lead to a slip and fall could be the surface finish, tile type, potential surface contaminants, and surface behavior. All of these factors should be considered when interpreting DCOF values along with anticipation of the conditions that are expected dependent on where the surface is being used.

2.3 Literature Review

The following publications help to outline an initial point for research to begin by providing valuable insight into the material selection, design selection, and procedures necessary for the evaluation of the mechanical properties of plantar skin. These topics ranges from material & design selection to valuable procedure insights necessary.

2.3.1 Experimental Investigation to Determine the Standardized Limit of the Coefficient of Friction for Slip Resistance during Walking

In 1996, Dr. Stefan Bönig completed his dissertation, “Experimental Investigation to Determine the Standardized Limit of the Coefficient of Friction for Slip Resistance during Walking.” The objective of Dr. Bönig’s dissertation was to determine the necessary limit of friction needed on a surface to reduce the risk of slip and fall accidents based upon conducted research. Within the scope of the project, force plates and human subjects were used walking across a variety of surfaces to measure the coefficient of friction present during slips and falls. Fifty subjects were selected to perform tests walking across numerous slippery to rough surfaces. The surfaces were configured in a variety of straight, curved, and inclined paths. Through statistical analysis and an acceptable level of risk, a value of 0.44 would be the proposed limit. This number was then compared verse other proposed limits suggested by other researchers. A limit of the coefficient of friction of 0.42 was then accepted by all thirty probationers at a subjective evaluation. This value would then be the accepted coefficient of friction in Germany, and would later help to lay the foundation for the ANSI A326.3 testing procedure, and the accepted 0.42 for flat level interior floors in the United States. [5]

2.3.2 Slip Resistance in Barefoot Areas

A paper was published in 2004 by the Swiss Federal Laboratories for Materials Science and Technology and the Swiss Competence and Coordination Centre for Accident Prevention written by Siegfried Derler, Freddy Kausch, and Roman Huber the issue of measuring slip resistance in barefoot areas was addressed. The researchers sought to answer whether an observable discrepancy between human ambulation and tribometer measurements differed with skin substitutes and which skin substitutes would produce reliable measurements via the use of a portable tribometer. Researchers noted how aside from previous standards in the United States for bathtubs and showers where plantar skin is simulated using medical-grade silicone[16,17], little other comparable substitutes are recognized. Meanwhile, in Germany and other countries located in Europe, the variable ramp incline is used to test wet barefoot areas[17][18][8]. Researchers state in their investigation about the performance of Lorica and felts that are commonly used noting that on smooth surfaces the substitutes produce reliable results comparable to that of plantar skin but differ on rougher surfaces. To help improve the results obtained, the researchers decided to focus on a new approach of coating already used materials like Lorica and felt with much softer plastics such as silicone elastomers. Through initial investigations, they discovered that some elastomers became apparent as potential candidates for substitutes where silicone recorded the smallest deviation from the data obtained from barefoot testing[17]. The study focused on the results from fourteen subjects (four females and 10 males) on twenty-eight different an impressive 3027 individual measurements were obtained. Subjects ranged in age from eight to sixty-three years old, weight between twenty-four to 108 kg, and shoe sizes from thirty-two to forty-five and a half. Surfaces were mounted atop a force plate and subjects were asked to slide their barefoot across the surface wetted with a solution while holding safety rails and keeping the other foot on a solid surface to prevent any accidents from occurring. Measurements were recorded by a computer at a sampling rate of 500Hz every two seconds. The sliding distance was between thirty and seventy centimeters with the pads of the foot being firmly and completely placed on the surface. Researchers noted that nearly all subjects carried the experiment out with the leg being slightly bent at an angle and two conducted the test with legs fully extended. Researchers also conducted a dry hand sensory classification experiment for each surface and determined that the results do not correlate one to one in comparison to the wet slip resistance of the surface. Researchers also had subjects conduct tests varying the amount of force applied to the surface and found that the friction coefficient for sliding decreased with the increase in load applied. Through statistical analysis and Spearman rank correlation coefficient, researchers obtained values that could be used to measure the slip resistance of the tested floor surfaces.

$$R_s = 1 - \left(\frac{6\Sigma d^2}{n^3 - n}\right) \qquad \text{[Eq. 2-11]}$$

After these values had been obtained, experiments using the FSC 2000, GMG, and Wuppertal Shoe Tester could be carried out with the desired plantar skin substitutes. The FSC 2000 was equipped with a Lorica slider and various materials where friction measurements were conducted on the same twenty-eight surfaces used in the human subject tests. As the same with the human trials, water with a 0.5% wetting agent was used as the medium between the surface and sensor material. A total of twenty different combinations were tested using materials such as cowhide, pigskin, silicone-board materials, silicone matter, and silicone foam rubber. After the tests had been conducted the research primarily focused on the most promising performances consisting of silicone materials due to the adequate performance of the material, a higher correlation of friction to plantar skin, and the capability to influence the frictional properties by adjusting the material thickness.

When testing with the 100 GMG was conducted, the researchers narrowed their samples to silicone sheet materials and silicone sponge rubbers. The results on the 100 GMG showed that the ideal material thickness that results in the best correlation between silicone and plantar skin occurred at a thickness of 1.5mm. These results not only correlated well to the results obtained from the human testing, but also to the values obtained from the FSC 2000.

For testing to be conducted on the Wuppertal floor and shoe Tester, a material thickness of 1.5mm was selected. Automatic measurements were taken across all twenty-eight of the flooring surfaces fifteen consecutive times for each surface. After each test, samples were checked for potential damage and replaced should prominent damage occur. The results obtained from the Wuppertal floor and shoe Tester correlated well to the results from the other experiments conducted. When graphed and analyzed, the results showed that Lorica and felt materials produced consistent higher results than that of silicone and planta skin. From the research and experiments conducted in this paper, a conclusion was reached that the use of silicone could be suitable for the frictional measurements of flooring materials especially when used together with Lorica. This information becomes relevant as a starting point for future testing to be done with the addition of microstructures to the silicone to determine if the error between silicone and plantar skin could be reduced further.

2.3.3 Bio-Inspired Textures for Functional Applications

A paper published by CIRP in 2018 written by Ajay P et al. covered the mechanical and functional properties of microstructures and surfaces that occur naturally ranging from plant species with super hydrophobicity properties to friction and drag reduction properties. For the purpose of this paper, the focus will be on hydrodynamic designs for drag reduction to provide potential designs to be tested in determining their effect on the DCOF. Researchers point out the benefits of managing frictional losses and note how the coefficient of friction between two surfaces (boundary lubrication) increases when there is direct contact between surfaces due to the dissipation of the load applied. However, even in a state of hydrodynamic lubrication, the coefficient of friction also steadily increases as well. Illustrated by the Stribeck curve, there is an area of interest as the Elasto-Hydrodynamic Lubrication (EHL) where there is a significant amount of elastic deformation that occurs on the surfaces and changes the form of the lubrication that separates the two contact surfaces. This area produces the lowest coefficient of friction. Researchers describe how shark skin is “an excellent example of a multifunctional surface as it can be used as a model for developing drag reduction schemes and low friction (tribological applications) surfaces”[2]. The researchers note how the riblet features of shark skin could be simplified in a 2-D riblet pattern that could easily be replicated and used for numerous designs in conjunction with different materials. Authors noted how besides the shark-skin designs, S. Molesta designs consisting of micro eggbeater features also showed an improvement in drag and friction reduction. Examples of the introduction of shark-skin designs into several manufacturing designs were noted consisting of research by Lufthansa airway in producing coatings to be used on aircraft, and Speedo Corporation in producing swimsuits. The most common process used in achieving these designs as noted by the authors is through laser surface texturing, where additional bio-inspired designs based upon snake-skin, tree frogs, and shark-skin have been used to improve the performance of everyday materials such as razors. This information helps to provide a basis for additional designs to be used and tested for the specific purpose of replicating the mechanical properties of plantar skin in regard to the DCOF.

2.3.4 Use of Biomimetic Hexagonal Surface Texture in Friction against Lubricated Skin

A paper published in the Journal of the Royal Society Interface in 2014 written by Alexey Tsipenyuk and Michael Varenberg covers the use of smooth contact pads in the shape of hexagons that have evolved in “bush crickets, tree and torrent frogs and mushroom tongued salamanders” [1]. This pattern has been replicated in elastomers and has been repeatedly tested in various conditions to evaluate the effect it has on friction. The paper discusses how patterned surfaces were created using negative molds and PVS. To make these small molds photolithographic patterning was used. These patterns were then affixed to a safety razor to be tested against human forearm skin. The skin temperature, room temperature, and humidity during testing were reported as 32°C, 24°C, and 45%. A total of fifteen measurements were taken across the same section of skin which was adequately covered by shaving foam with a normal load of 2N at a velocity of three millimeters per second across a total distance ranging from twenty-five to thirty millimeters. The tangential force was recorded, the forearm cleaned from any potential contaminants, the foam was reapplied, and the test was repeated. The authors then proceed to describe the diameter, thickness, height, and center distance of each pattern that was tested. The results from the published paper address optimizing the drainage system present to reduce the amount of lubricating fluid present while achieving an optimal surface contact area. The paper describes an optimal channel drainage efficiency to be used to increase the friction. The design that performed the best optimized the ability to drain the lubricant while maintaining an adequate contact area. By reviewing this paper, valuable insight into decreasing friction is obtained to be used in the creation of designs since previous research has shown that silicone performs slightly higher than plantar skin. These factors will be considered when creating designs to be used during testing.

2.3.5 ANSI A326.3 Procedure

Because of the selection to use the walkway tribometer produced by Regan Scientific Instruments, it is important to review any related literature and procedures to the operation of the device. ANSI A326.3 states a standardized procedure for the operation of the device for use in flat level interior spaces to assess the slip resistance of surfaces. The following is a summary of the A326.3 procedure. Procedures for the use of the BOT-3000E should always start with the assessment of the SBR rubber sensor to be used and evaluation should be made on the state of wear on the surface. Should the sensor need to be reconditioned, it should be inserted correctly into the reconditioning tool provided with the appropriate sandpaper. Sanding the SBR rubber is essential in ensuring the appropriate contact surface and should be regularly checked and reconditioned. Any excess material that may be present on the sandpaper or sensor should be removed via a dry stiff brush. Reconditioning should be repeated until the sensor presents no visible wear lines. The next step is to ensure that the BOT-

3000E passes its strain verification. The verification mass should be inserted into the bottom of the BOT-3000E while it is perpendicular to the surface. Once the verification procedure completes and results in a passing grade, validation of the sensor is necessary. The reference surface should be cleaned and be free from debris using an approved cleaner to fully remove and potential contaminants and then thoroughly rinsed. A path should be created using 0.05% sodium lauryl sulfate water solution (SLS). This path should extend throughout the entire testing distance and should be wide enough to ensure that the sensor remains in the solution during the entirety of the test. A soft bristle brush can be used to spread the solution. One measurement should be taken, and then the BOT should be rotated 180° to obtain another measurement. Leave the BOT on the surface until the entire distance has been covered. Average the two values obtained from the test that should be within the tolerance of ±0.03 of the value stated for the reference surface. Should the value not be to tolerance, repeat the entire testing procedure including reconditioning of the sensor and surface. If it remains outside the tolerance, the sensor should be discarded and a new sensor should be used. Should the SBR sensor thickness fall below two millimeters, the sensor should be discarded and replaced. The validation procedure should be repeated to ensure the new sensor passes.

Once an appropriate sensor has been obtained testing on the surface in question can be commenced. All surfaces in question should be cleaned with an approved cleaner until all surface contaminants have been removed. Ensure the surface to be tested in flat and level, if not place the surface on a solid surface and ensure there is enough material to accommodate the travel distance and wheels of the BOT as it traverses the surface in question. Enough 0.05% SLS solution should be applied to ensure the sensor remains in the solution throughout the entire path and covers the entire width of the sensor but does not interfere with the traction for the wheels. Once the path has been created, set the travel distance to ten inches or to the longest possible distance for the surface in question. Using the provided directions on the BOT screen, complete the entire test by taking a total of four measurements across the different points of the surface in question. The first measurement should be made then the BOT should be rotated 180° traverse the same path, replace the SLS solution as needed. One these two measurements have been completed, remove the SLS solution rotate the device 90° re-wet the surface and make the third measurement. Once this process has been completed, rotate the bot 180° to take the fourth measurement. The 90° rotation should occur at the end of the second measurement, but there is no specific reason for this as there should be a little variation of the DCOF across the surface in question. This procedure is then repeated for two additional locations across the surface. The sensor should be evaluated after each measurement to determine if reconditioning is necessary. A total of twelve measurements will be taken for a total of 3 averages. The sensor should then be rechecked after testing on the validation surface, should it fall outside the stated range the tested results should be evaluated to determine a potential error if not error is found the results should be discarded and the process should be repeated. This procedure states that a value of 0.42 or higher is adequate for surfaces expected to be walked upon while wet, and any value below this threshold should be properly maintained and kept dry. However, a value of 0.42 may not be necessary for all surfaces, and the specific use should be considered when making this determination.

2.3.6 Relevance

These papers selected help to provide a starting point for research to begin. Section 2.3.1 helps to establish a starting point for assessing walkway safety and steps necessary for outlying a standardized limit of coefficient of friction necessary to reduce the potential for slips and falls. Section 2.3.2 establishes a starting point for material selection showing that the use of soft polymers with sufficient deformation characteristics similar to human skin can be used and closely replicate the results. Section 2.3.3 provides information in the applications of specific biomimetics and potential designs that could be applied. This section also covers the uses of particular designs along with similar research that is being conducted. Section 2.3.4 shows the practical application of biomimetics is possible and can yield desirable results in their use. Section 2.3.5 shows established standards already in place for assessing walkway safety and procedures relevant for testing. This helps in providing an outline for potential standards in assessing walkway safety for bare feet.

CHAPTER 3

METHODOLOGY FOR FABRICATION AND TESTING OF BIOMIMETIC STRUCTURES

The following section covers the principle behind printing via DLP, water contact angle measurements, and surface roughness measurements. The design of experiments and relevant information are also covered. This covers current subject knowledge relevant to the experiment, variables to be studied, a method for replication, and method for randomization, the applicable design matrix, and planned method of statistical analysis. Furthermore, results obtained from an on-going surface treatment study and the obtained results from experimentation with ceramic-polymer and soft polymer materials.

3.1 Direct Light Processing Principle

The most common resin-based 3D processes currently available are stereolithography (SLA) and direct light processing (DLP). The main advantage to using a resin-based 3D printer is the ability to print isotropic, exceedingly accurate, and impermeable designs with a comprehensive variety of obtainable materials with different mechanical properties and smooth external finishes. Due to SLA having a longer average build time for prototypes, DLP was selected to be used. The DLP equipment being used is a desktop Vida model from Envisiontec. DLP operates by exposing liquid resin to a light source to create very thin solid layer that stacks to create the desired shape. The tanks where the liquid resin resides has a clear bottom for the light source to project through. DLP works by lowering the build platform into the resin tank to the specific z-height to acquire the necessary layer thickness. Then, the projector exposes an image of the print layer into the resin tank to simultaneously cure all the desired points. As shown in figure 3-1, DLP uses a light source that is then directed towards the DLP chip via the precision optics used. This light is then projected through the lens into the desired coordinates curing the entire layer at once. This factor is the reason why DLP can print designs faster than SLA, which uses a laser to profile the entire printed layer. However, because DLP uses a projector that is a digital screen, each layer is an image composed of pixels, which then result in a three-dimensional layer of small rectangular cubes called voxels. This results in a lower resolution than SLA with the benefit of rapid prototyping. DLP and SLA can offer some of the highest resolution in the z-axis (thinnest printable layers).

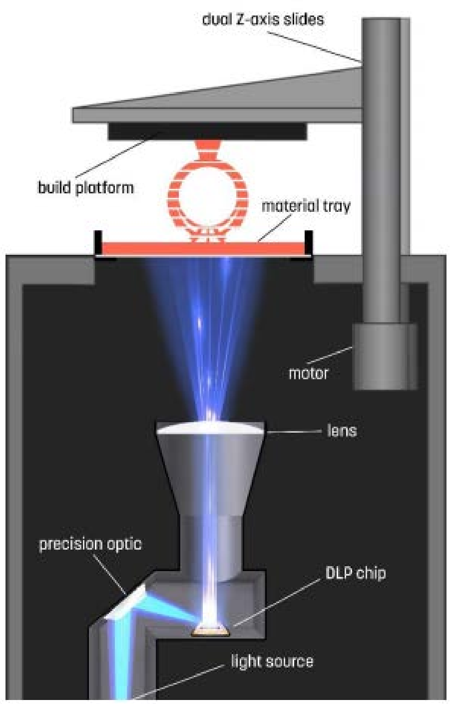

Figure 3-1: Direct light processing printing diagram via Envisiontec [19]

The XY resolution for the Vida desktop printer is seventy-three micrometers or approximately 0.0029 inches. The Z resolution is twenty-five to 150 micrometers or

0.001 to 0.006 inches. The light source for the Vida desktop is an industrial UV LED. Finally, the build platform is 140 x 79 x 100 mm or 5.5” x 3.1” x 3.95”. The resolution of the project being used is 1920 x 1080-pixel resolution. Direct light processing will be utilized to determine feasibility of the designs to be tested. The method provides accurate designing with a quick printing process versus other methods. This was chosen to reduce build times and maintain a sufficient surface finish versus stereolithography which offers higher precision and accuracy at the cost of longer build time. Voxels attribute to the lower surface finish and detail capability inherent to direct light printers. Another major benefit of using DLP is the availability of an extensive range of materials to print with, each offering benefits of specific and desirable mechanical properties. Initial research was conducted using a ceramic-polymer as the printing material. This resin is a harder material due to ceramic particles added to the resin. The ceramic-polymer has a high accuracy printing resolution, nevertheless due to the hardness, a softer polymer material was selected for final designs after initial feasibility testing was done. Because the new material selected is a softer polymer, the ability for it to more precisely replicate mechanical properties similar to plantar skin are higher, as shown from previous research conducted in section 2.3.2. An image of the DLP printer and curing oven used is shown in Figure 3-2.

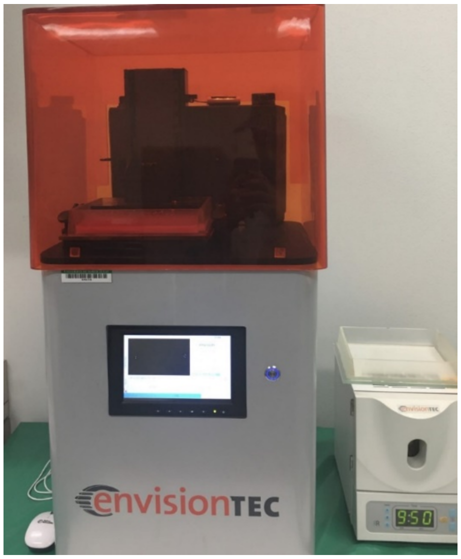

Figure 3-2: Printer (left) and curing oven (right)

3.2 Water Droplet Contact Angle Equipment Principle

Contact angle is a common way to measure the wettability of a material. This refers to how the liquid spreads or the ability for the liquid to spread across the solid surface and form boundaries when deposited. Surfaces that have a high degree of wettability typically show low angle values when the contact angle is measured, while surface that have a low degree of wettability typically show angles that are much higher. This is done via the use of a modified Young's equation. The equilibrium contact angle can be calculated and will reflect data relative to the strength of the molecular interaction between the solid, liquid, and vapor. This will be utilized for the treatment study conducted to assess what impact the treatments may have on the surface and how the untreated surfaces wettability affects the application of the treatment. If the contact angle is less than ninety degrees the liquid will spread and wet the surface. If the liquid is greater than ninety degrees the liquid will stay on the surface as a bead. This will impact the ability for treatments suspended in a liquid to be properly and uniformly applied to a surface. An image of the equipment is provided in Figure 3-3

Figure 3-3: Contact angle measurement equipment

3.3 Tactile Surface Profilometer Principle

A tactile profilometer is a valuable piece of equipment for assessing the roughness of a surface and used to extract topographical information regarding that surface. Some profilometers can do single points, a scan along a line, or a three-dimensional rendering of the scan. This is useful as it will provide information regarding the step heights and surface roughness. The tactile profilometer used requires a force feedback and to physically be touching the surface in order for it to work. This makes the profilometer very sensitive to soft surfaces and vibrations however it does provide high Z resolution. The downside to using a tactile profilometer is it takes time to traverse the surface using the set parameters and must maintain contact with the surface and can be slow at times. The stylus that is used for the measurements is typically conical with a spherical tip at the end ranging anywhere from two micrometers up to ten micrometers with taper angles varying from sixty degrees to ninety degrees. For the profilometer used the taper angle is sixty degrees. It is important that the correct sampling length and evaluation length is used based on the expected surface roughness. The following table can be used to help determine what parameters should be used. The tactile profilometer will be used to test the surface roughness of the samples from the treatment study and the effect the treatments may have on the samples.

Table 3-1: Sampling and evaluation length for surface roughness parameters

Ra (μm)	Sampling length (mm)	Evaluation length (mm)
0.006 < Ra ≤ 0.02	0.08	0.08
0.02 < Ra ≤ 0.1	0.25	0.25
0.1 < Ra ≤ 2	0.8	0.8
2 < Ra ≤ 10	2.5	2.5
10 < Ra ≤ 80	8	8

Figure 3-4: Tactile profilometer

3.4 Design of Experiment

3.4.1 Current Subject-Matter Knowledge

This section covers current knowledge related to the subject in question, this will help to aid in guiding new knowledge attained.

- The coefficient of friction is the ratio of the frictional force to the normal force.
- The main contributing factors to wet friction is adhesion and hysteresis, but at low velocities, friction is mostly attributed to adhesion.

- Typically, static friction is higher than dynamic, but this does not always occur.
- Different methods exist for measuring the dynamic coefficient of friction, this consists of the:
    - Drag sled – measures the ratio of frictional force to the normal force
    - Pendulum – measures energy loss due to frictional forces
    - Variable angle ramp – measures the coefficient of friction present at a slip.
- Acceptable coefficient of correlation between methods averaging
    - Above .75 in SAE 10W-30 engine oil.
    - Above .65 in water+SLS solution [specific correlations provided in the method of coefficient correlation section.

3.4.2 Variables to be Studied

This section differentiates between the variables that are present during the experiment. The factors of interest are also listed along with background variables.

1. Response variables – Dynamic coefficient of friction
2. Factors – Microstructure design, material, wetting agent
3. Background Variables – surface type (natural stone, porcelain, ceramic, etc.)

3.4.3 Method for Replication

This section covers the method for replicating the experiment to assess the extent of experimental error that may have occurred during the initial testing. This will be done through a variety of methods. For the treatment study repeated observations of the response variables will be used. Four measurements across three different locations on the tiles while using the walkway tribometer will be selected for testing per ANSI A326.3 procedure. Per each tile set twelve measurements representing the coefficient of friction for an assessment of the surface will be averaged together. For the biomimetic study three samples of natural stone, porcelain, and ceramic will be used for the experiment and randomly selected. After experimentation has been completed with the tribometer, the same experiment can be replicated using the same experimental parameters with a different BOT. Results obtained from testing the same surfaces should be within statistical error of the values obtained from the first set of testing. Additional surfaces can be tested and added as flooring trends change to be tested under the same experimental criteria. The BOT3000E automatically generates a report with relevant information such as temperature, relative humidity, and testing distance. Obtained results are also included along with a graphical representation of the measurements during testing. This is valuable as an evaluation of the graph can indicate potential signs of inconsistency during the test. Ideal graphs should peak at the beginning indicating the static coefficient of friction, then be relatively smooth and consistent horizontally. Any drastic peaks can indicate an inconsistency that affected the measurement.

3.4.4 Method for Randomization

The order in which the designs will be tested and the order of the surfaces to be tested will be randomized through the use of Minitab in order to eliminate any potential bias. Three different brands/types of porcelain, ceramic, and natural stones will be selected to be used for the experiment. Additional surfaces can be added and tested at if the need arises.

3.4.5 Design Matrix

The design matrix shown will be the outline for the data to be collected as shown in Table 3-2. Additional materials and tribometers can be used to verify the values.

Initially, these surfaces will be untreated, but additional research should be conducted in the treatment of tile surfaces and the effect that may occur to change the DCOF. Each design will receive an averaged value that occurs from the several measurements taken by the tribometers across the tile surface. The order of testing for the designs will be randomized through the use of Minitab. This was done by inputting all the designs mentioned above into Minitab. Then calc>random data > sample from columns. The number of rows to sample is the number of designs (11). The same procedure was repeated for the testing order of the tile samples. The order of the designs to be tested will be the same throughout testing and the same is true for the order of the tile samples. The obtained testing order for the designs

1. Concentric circles
2. Justified cylinders
3. Offset cylinders
4. Offset hexagons
5. Parallel lines
6. Perpendicular lines
7. Solid
8. Perpendicular offset sharkskin
9. Parallel justified sharkskin
10. Perpendicular sine wave
11. Parallel sine wave

Table 3-2: Design matrix

BOT or equipment used	
Material 1	
Tile Type	**Designs to be tested and separated**

Porcelain 1											
Porcelain 2											
Porcelain 3											
Natural stone 1											
Natural stone 2											
Natural stone 3											
Ceramic 1											
Ceramic 2											
Ceramic 3											
Other 1											
Other 2											
Other 3											

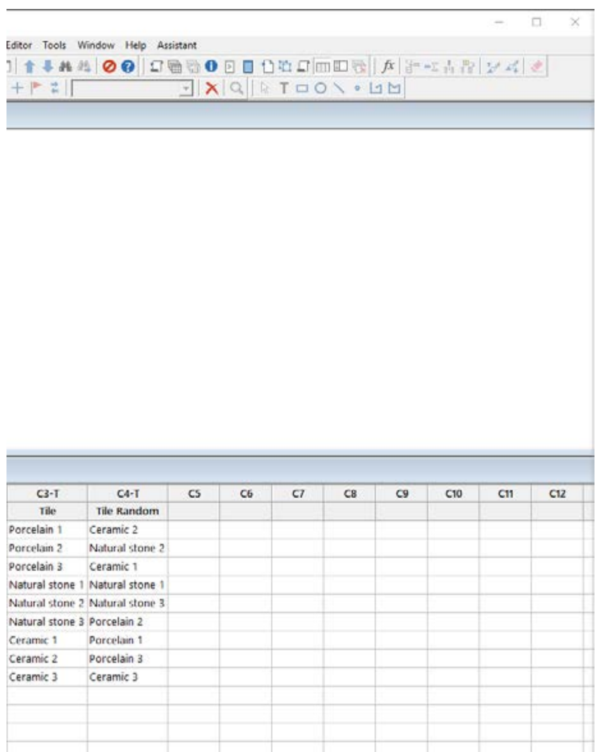

C3-T	C4-T	C5	C6	C7	C8	C9	C10	C11	C12
Tile	Tile Random								
Porcelain 1	Ceramic 2								
Porcelain 2	Natural stone 2								
Porcelain 3	Ceramic 1								
Natural stone 1	Natural stone 1								
Natural stone 2	Natural stone 3								
Natural stone 3	Porcelain 2								
Ceramic 1	Porcelain 1								
Ceramic 2	Porcelain 3								
Ceramic 3	Ceramic 3								

Figure 3-5: Tile random sample

1. Ceramic 2 – beige ceramic
2. Natural Stone 2 – polished black granite

3. Ceramic 1 – white viena ceramic
4. Natural stone 1 – polished white marble
5. Natural stone 3 – travertine
6. Porcelain 2 – polished porcelain
7. Porcelain 1 – textured glazed porcelain
8. Porcelain 3 – polished white porcelain
9. Ceramic 3 – slate ceramic

The order in which the tile surface will be tested was randomized as well to reduce potential bias in the selection of the surfaces.

3.4.6 Planned Method of Statistical Analysis

Any unusual outlying DCOF measurements will be investigated in regard to the structure and material used. This can consist of irregularly high or low measurements not anticipated or similar to measurements of the same type. For the treatment study, a relevant analysis of the variance will be used to determine whether the method, surface, or treatment had a discernable effect on the response variable. A Fisher pairwise comparison at the 95% confidence will be utilized to compare the different treatments, measurement methods, and surfaces. An appropriate analysis of variances will be utilized for the biomimetic study to determine whether the design and tested surfaces have a statistically discernible effect on the response variable. A Tukey pairwise comparison will be done to determine if any of the designs are statistically discernable from one another and the barefoot testing values. Designs that are not statistically discernable from the barefoot values would indicate a positive relationship between the proposed design and the measured barefoot values.

3.5 Treatment Study

The following section will cover results obtained from an on-going experimental study to investigate the effect conventional treatments may have on the dynamic coefficient of friction on different surfaces. Treatments were selected to be applied to four types of tile surfaces: polished and glazed textured porcelain, natural stone, and vinyl composite tile or luxury vinyl tile. Manufacturers of the treatments were contacted for application of the product; if the manufacturer opted to not apply the treatments then the treatment was applied via the present researcher. ANSI A326.3 testing procedure was utilized during the experiment. The collected data resulted from four measurements at three points on the surface of the tile. These data points for each surface set were collected and then averaged together to obtain a mean value for the DCOF of the surface and treatment type. The study was done with standardized equipment, sensors, and surfaces under known conditions. Per ANSI A326.3 the standardized limit of DCOF for a surface anticipated to be walked upon while wet, should have a wet dynamic coefficient of friction value > 0.42. Measurements of untreated samples were obtained in order to compare what effect treatments may or may not have on the DCOF. The following subsections will cover the efficacy of commercially available product's performance on flooring. Treatment effects will be measured via drag sled, pendulum, and ramp methods. Surface roughness measurements of the different treatments and surface will be tested. Ra values for each surface will be obtained. Three samples from every treated surface will be collected for testing and each sample will be measured three times along the middle, left, and right sides of the sample. A Mitutoyo tactile surface profilometer is used for the measurements. For the polished surfaces like polished porcelain and polished black granite, the sampling length will be 0.8mm. For the VCT and textured glazed porcelain the sampling length will be 2.5mm. Additionally, samples will be tested using a water contact angle measurement equipment in order to determine the relative wettability of the surface. For each surface two measurements will be taken for the contact angle θ for the left side and right side of the droplet. The mean, height, and width of the droplet will also be provided from the measurements. This study is important in determining whether treatments can change the measurable DCOF values as any potential designs that have a consistent relationship with plantar skin will need to be tested on treated surfaces at some point to ensure no large difference occurs.

3.5.1 Drag Sled Results

The following data was obtained from measuring the DCOF of a surface while using the BOT3000E. Measurements were taken before treatment applications and after to compare any possible effects. The treatments are labeled as A, B, C, D, and E. These treatments were tested on four surfaces using the ANSI A326.3 procedure, the three obtained values were then averaged together to achieve the numbers presented in Table 3-3. Surface VCT was omitted for the statistical analysis as some treatments were not intended to be used on that type of surface. The average of all the treatments for each surface was taken for comparison. Per ANSI A326.3, 0.05% SLS solution was used as the lubricant during testing of the surfaces. SLS was laid down to ensure the sensor would remain within the solution throughout the ten-inch measurement. The boxplot and mean bar chart for the drag sled show the highest mean value is for treatment B closely followed by treatment D.

Table 3-3: Drag sled treatment results

-	Untreated Control	A	B	C	D	E	Mean
Polished porcelain	0.19	0.09	0.59	0.32	0.31	0.26	0.335
Polished black granite	0.25	0.29	0.36	0.35	0.33	0.37	0.365
VCT	0.4	0.27	0.48	N/A	0.41	N/A	0.4275
Textured glazed porcelain	0.45	0.24	0.62	0.5	0.57	0.57	0.525

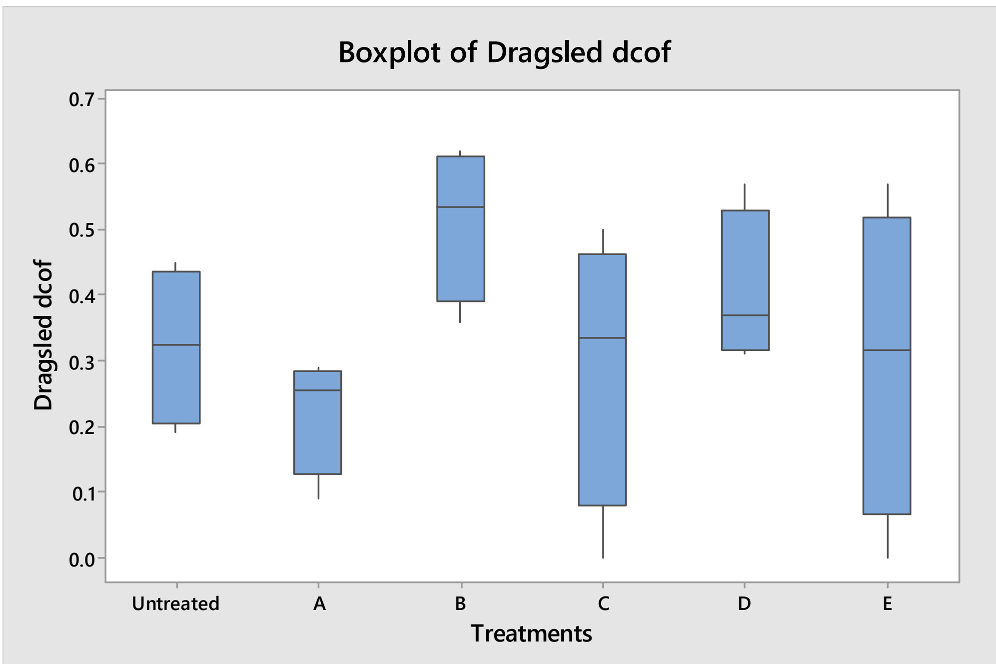

Figure 3-6: Boxplot of treatments DCOF values using a drag sled

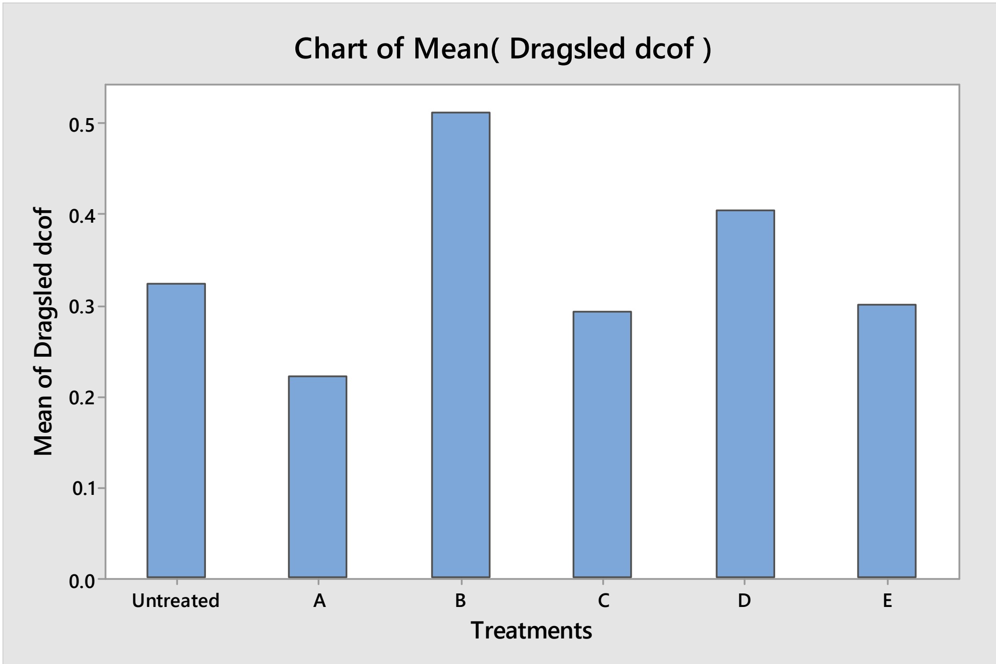

Figure 3-7: Bar chart of mean treatment DCOF values using drag sled

3.5.2 Pendulum Results

The following data was obtained from measuring the DCOF of a surface while using the Knightcott surface solutions pendulum and following the relevant testing method. Surfaces were tested using a prepared type 96 rubber slider with the surfaces being tested using a skidding distance of approximately 123-125mm and distilled water as the lubricant. Again, some treatments were not intended for use on VCT tile and these are omitted. The obtained values for the untreated control appear to be very close to the values obtained by using the drag sled method. However, the mean values across the polished porcelain and polished black granite for all treatments appear to be lower than the mean values for the drag sled method. The boxplot and bar charts for the pendulum show the highest median value is for treatment B closely followed by treatment D.

Table 3-4: Pendulum treatment results

	Untreated Control	A	B	C	D	E
Polished porcelain	0.21	0.22	0.37	0.19	0.29	0.14
Polished black granite	0.20	0.27	0.21	0.15	0.13	0.12
VCT	0.38	0.23	0.35	N/A	0.37	N/A
Textured glazed porcelain	0.47	0.38	0.76	0.65	0.67	0.79

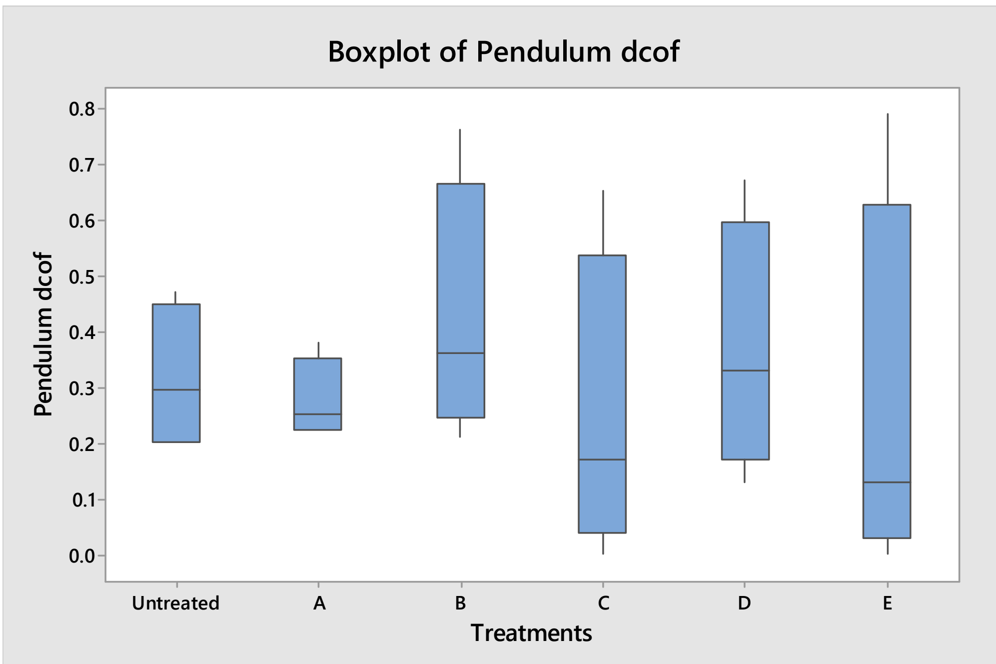

Figure 3-8: Boxplot of treatments DCOF using pendulum

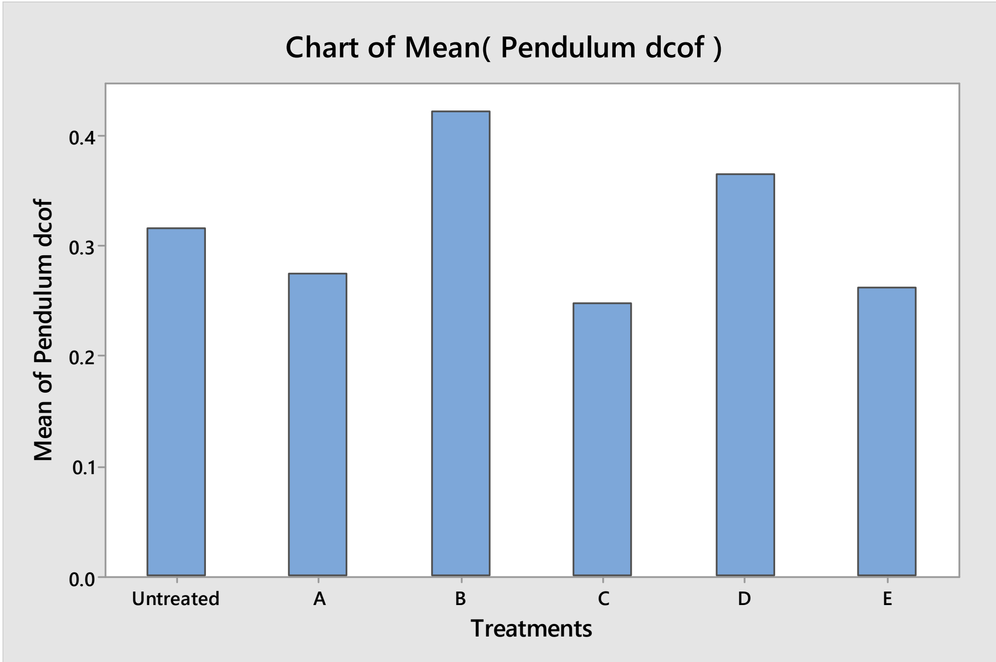

Figure 3-9: Bar chart of mean treatment DCOF values using pendulum

3.5.3 Variable Angle Ramp Results

The following data was obtained from measuring the DCOF of a surface while using the variable angle ramp method and following the relevant testing method DIN 51131. The variable angle ramp has two associated standards. One standard utilizes 10W-30 SAE oil as a lubricant and the other utilizes 0.1% sodium lauryl sulfate as a lubricant. Additionally, a standardized footwear per the method was used while the test subject walked across the surface. For these results the 0.1% SLS method was used to obtain the values in Table 3-5. The textured glazed porcelain appears to be much higher in this method than the other two. However, mean values for the treatments across the polished porcelain and polished black granite appear to be similar to the results obtained from the drag sled method. The values obtained from the variable angle ramp show on average that treatments B and D performed better than other treatments.

Table 3-5: Variable angle ramp results

	CONTROL	A	B	C	D	E
Polished porcelain	0.19	0.36	0.61	0.6	0.59	0.25
Polished black granite	0.29	0.33	0.39	0.41	0.42	0.39
VCT	0.56	0.32	0.57	N/A	0.95	N/A
Textured glazed porcelain	0.60	0.42	0.91	0.98	0.97	0.86

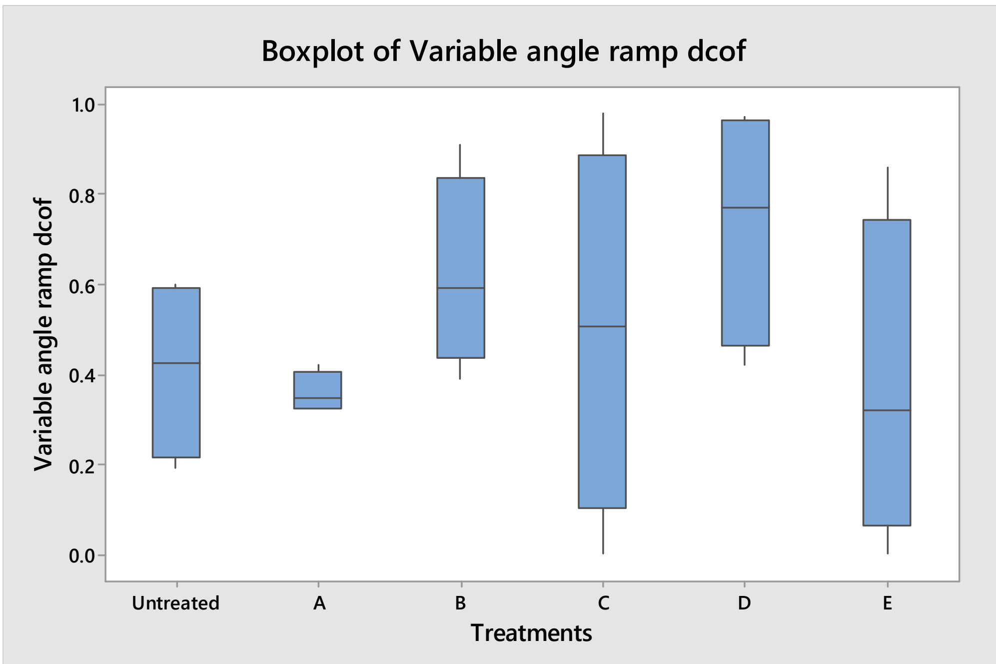

Figure 3-10: Boxplot of treatment DCOF values using variable angle ramp

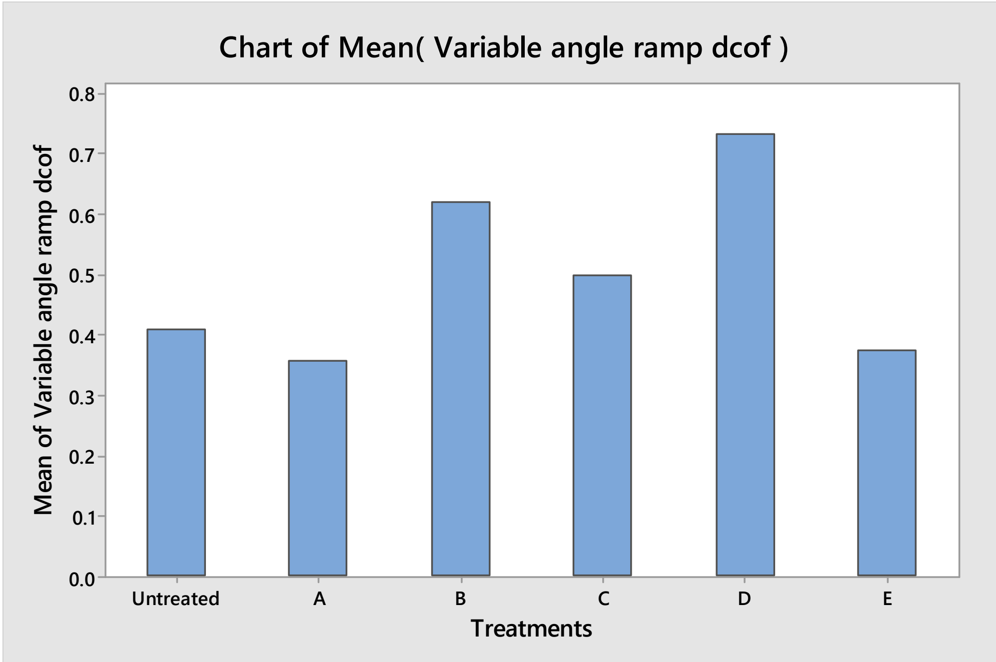

Figure 3-11: Mean bar chart of treatment DCOF values using variable angle ramp

3.5.4 Water Contact Angle

This section will cover the results obtained from the water contact testing. This will provide background into the wettability of the surfaces before treatment and the wettability of the surface's posttreatment. If a surface has a low wettability it is said to be hydrophobic, and surfaces with a high wettability are said to be hydrophilic. This is important as it will impact the ability for liquid based treatments to properly and evenly spread across the surfaces.

Table 3-6: Water contact angle

	Left θ	Right θ	Mean θ	Height	Width
Untreated					
Polished porcelain	94.10	95.40	94.80	0.97	3.53
Polished porcelain	93.40	95.00	94.20	0.95	3.53
Polished black granite	66.60	68.80	67.70	0.85	4.41
Polished black granite	65.00	67.40	66.20	0.82	4.41

	Left θ	Right θ	Mean θ	Height	Width
VCT	72.60	72.70	72.60	1.34	4.34
VCT	73.60	72.60	72.90	1.00	4.34
Textured glazed porcelain	47.50	40.90	44.20	0.67	3.64
Textured glazed porcelain	42.40	40.20	41.30	0.82	5.37
TREATMENT A					
Polished porcelain	100.80	97.30	99.00	1.60	3.54
Polished porcelain	98.20	94.80	96.50	1.60	3.62
Polished black granite	65.00	64.60	64.80	1.19	4.59
Polished black granite	57.60	60.40	59.00	1.11	4.86
VCT	65.40	75.40	70.40	1.26	4.47
VCT	70.00	68.50	69.30	1.31	4.60
Textured glazed porcelain	64.20	63.80	640.00	1.04	4.57
Textured glazed porcelain	73.90	62.50	68.20	1.11	4.76
TREATMENT B					
Polished porcelain	88.90	87.50	88.20	1.54	3.78
Polished porcelain	86.00	85.50	85.70	1.53	3.76
Polished black granite	45.10	44.90	45.00	1.02	5.25
Polished black granite	50.40	49.10	49.80	1.07	5.31
VCT	57.20	55.30	56.30	1.21	4.86
VCT	70.50	70.50	70.50	1.42	4.57
Textured glazed porcelain	25.00	22.80	23.90	0.48	7.62
Textured glazed porcelain	19.60	17.30	18.50	0.42	7.15
TREATMENT C					
Polished porcelain	94.40	96.80	95.60	1.63	3.60
Polished porcelain	119.40	109.40	114.40	1.40	3.57

	Left θ	Right θ	Mean θ	Height	Width
Polished black granite	52.40	52.60	52.50	1.00	4.95
Polished black granite	51.20	49.60	50.40	1.01	5.19
VCT					
VCT					
Textured glazed porcelain	38.00	19.00	29.00	0.44	6.20
Textured glazed porcelain	65.70	64.90	65.30	1.06	4.93
TREATMENT D					
Polished porcelain	101.10	100.80	101.00	1.24	3.16
Polished porcelain	146.50	128.60	137.70	1.39	3.12
Polished black granite	73.70	68.50	71.10	1.01	4.71
Polished black granite	62.40	58.50	60.50	1.10	4.64
VCT	65.40	64.60	65.00	1.24	4.08
VCT	71.40	67.90	69.60	1.25	3.88
Textured glazed porcelain	45.20	45.00	45.10	0.80	4.83
Textured glazed porcelain	49.30	49.10	49.20	0.85	4.46

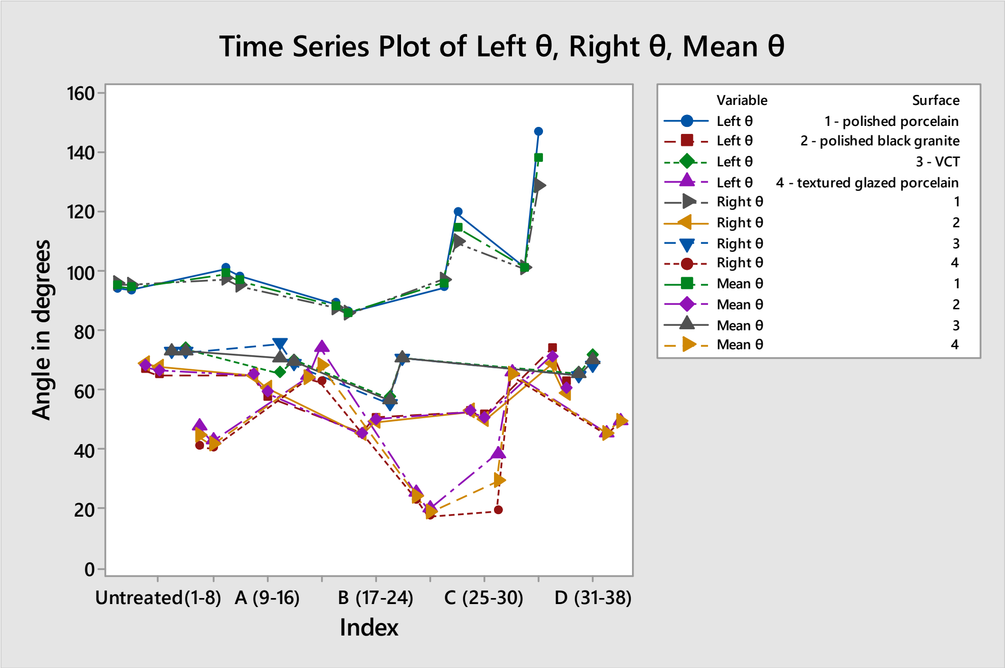

Figure 3-12: Line graph of left, right, and mean angles from contact angle measurements

By comparing the contact angle to the DCOF we can see that treatments that raise the DCOF also cause a decrease in the contact angle. Treatments that were not as effective in raising the DCOF did not increase the wettability of the surface. This would agree with the DCOF testing as the more a liquid can spread across the surface the more surface-to-surface contact that can occur. The polished porcelain surface had a low DCOF measurement and a high angle of contact for the water droplet. These measurements show the intensity of the phase contact between the water and the tile surfaces. Effective treatments that increased the DCOF significantly also increased the wettability of the surfaces as well.

3.5.5 Surface Roughness

Surface roughness was also tested on the treated surfaces in order to evaluate what sort of phenomenon is occurring due to the treatments. The surface roughness of the untreated samples was lower than the surface roughness of the treated samples.

However, the measurements for each sample was not always consistent with some samples displaying measurements lower than others within the same category. This could be due to uneven treatment applications and the inability for the treatment to uniformly spread across the sample surface. The less effective the treatment the less the surface roughness is impacted. Most available treatments for increasing the DCOF of surfaces are typically acid based and etch a new surface profile into the sample. For the polished surface a sampling length of 0.8mm was used and an evaluation length of 0.8. For the VCT and granite surface 2.5mm sampling length and 2.5mm evaluation length was used. Samples were collected from each type of surface and tested along the left, middle, and right sides of the samples as shown in Figure 3-13 and Table 3-7.

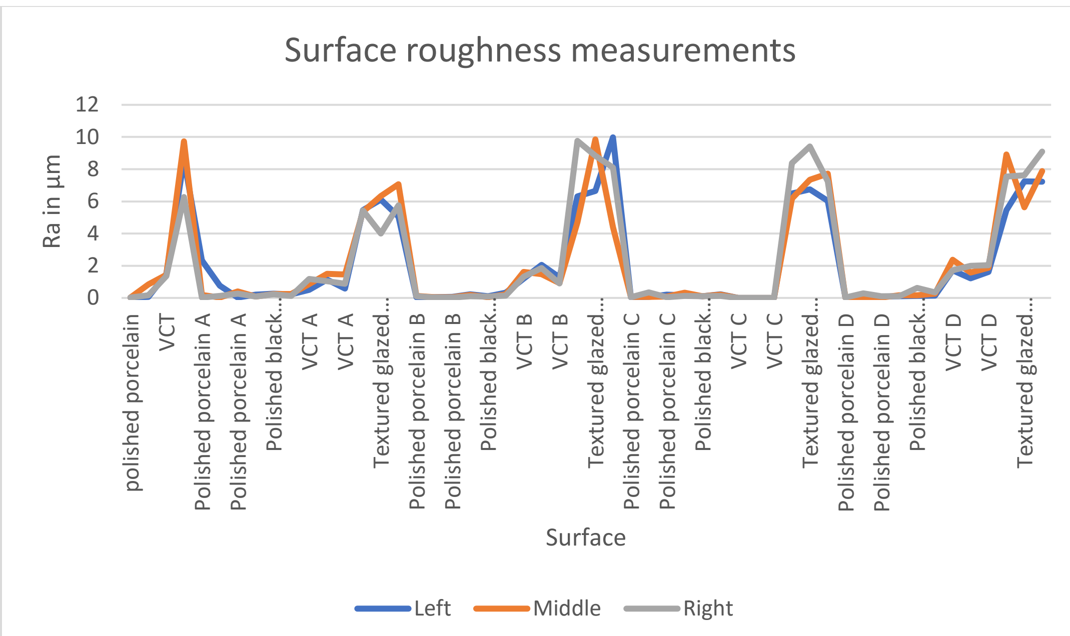

Figure 3-13: Surface roughness profile of samples

Table 3-7: Surface roughness results (µm)

	LEFT	MIDDLE	RIGHT
UNTREATED			
Polished porcelain	0.03	0.02	0.02
Polished black granite	0.06	0.85	0.16
VCT	1.5	1.44	1.35
Textured glazed porcelain	8.64	9.73	6.28

	LEFT	MIDDLE	RIGHT
TREATMENT A			
Polished porcelain 1	2.33	0.18	0.03
Polished porcelain 2	0.77	0.02	0.13
Polished porcelain 3	0.02	0.4	0.27
Polished black granite 1	0.21	0.09	0.08
Polished black granite 2	0.26	0.24	0.22
Polished black granite 3	0.23	0.24	0.12
VCT 1	0.51	0.87	1.17
VCT 2	1.13	1.5	1.03
VCT 3	0.59	1.46	0.89
Textured glazed porcelain 1	5.45	5.35	5.44
Textured glazed porcelain 2	6.12	6.32	4.01
Textured glazed porcelain 3	5.06	7.06	5.75
TREATMENT B			
Polished porcelain 1	0.04	0.12	0.1
Polished porcelain 2	0.05	0.04	0.03
Polished porcelain 3	0.06	0.04	0.03
Polished black granite 1	0.22	0.18	0.11
Polished black granite 2	0.11	0.05	0.08
Polished black granite 3	0.33	0.22	0.15
VCT 1	1.2	1.62	1.31
VCT 2	2.05	1.48	1.85
VCT 3	1.28	0.92	0.9
Textured glazed porcelain 1	6.31	4.69	9.76
Textured glazed porcelain 2	6.65	9.85	8.83
Textured glazed porcelain 3	9.98	4.41	8.1
TREATMENT C			
Polished porcelain 1	0.04	0.06	0.04
Polished porcelain 2	0.06	0.07	0.35
Polished porcelain 3	0.2	0.09	0.05
Polished black granite 1	0.17	0.32	0.12
Polished black granite 2	0.11	0.11	0.1
Polished black granite 3	0.23	0.2	0.13
VCT 1			
VCT 2			
VCT 3			
Textured glazed porcelain 1	6.48	6.17	8.38
Textured glazed porcelain 2	6.75	7.34	9.42
Textured glazed porcelain 3	6.04	7.72	7.24
TREATMENT D			
Polished porcelain 1	0.02	0.02	0.02
Polished porcelain 2	0.02	0.03	0.29

	LEFT	MIDDLE	RIGHT
Polished porcelain 3	0.09	0.03	0.11
Polished black granite 1	0.1	0.17	0.11
Polished black granite 2	0.12	0.17	0.62
Polished black granite 3	0.14	0.26	0.34
VCT 1	1.71	2.38	1.71
VCT 2	1.22	1.58	1.99
VCT 3	1.62	1.87	2.04
Textured glazed porcelain 1	5.46	8.92	7.54
Textured glazed porcelain 2	7.24	5.63	7.63
Textured glazed porcelain 3	7.23	7.88	9.1

Treatment C was not intended for use on vinyl composite floors, therefore the treatment was not applied. Additionally, testing on treatment E is still in progress and the samples were not available for surface roughness or water contact angle testing. Uneven treatment applications can be evident by the differences that occur in the measurements. An example of this is evident in treatment B on the textured glazed porcelain 1, which has a large range in the measured values. Treatments that were effective in increasing the DCOF also increased the surface roughness of the samples. However, application of the treatments and measurements show that the entirety of the surfaces were not evenly treated. Some samples exhibited drastic changes in the surface roughness while in the same sample another measurement showed little to now change. Even and uniform application of the treatment is key in producing changes in the DCOF.

3.6 Preliminary Testing with Ceramic-Polymers

As mentioned before, ceramic-polymer resin was selected due to the high resolution of the material. The initial spacing test for this polymer is show in Figure 3-14

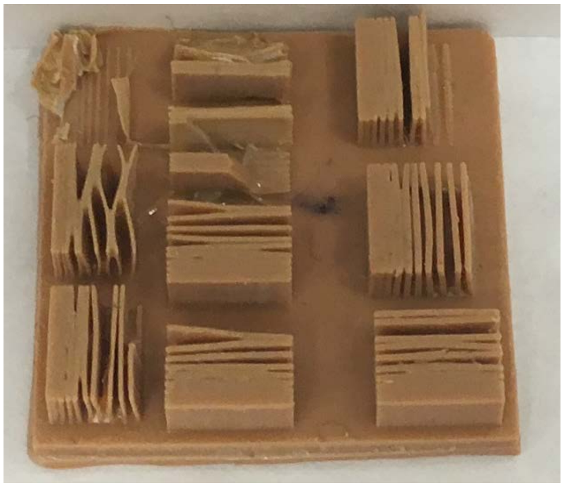

Figure 3-14: Spacing for ceramic-polymer photo

Initial designs showed an inability for residual resin caught between narrow spaces to properly drain during print layer removal causing significant errors in printed results. Testing into the specific printing spacing was conducted to evaluate the capability of the equipment to print at the necessary levels. Additionally, research into the minimum line thickness for sufficient support was included in this experiment. Results pictured above in Figure 3-14, lines with a thickness of <0.25mm or 250μm showed inadequate support causing significant deformities. Through analysis of the space between prints, a distance of at least <0.30mm or 300μm was needed for proper drainage to be achieved. This aided in providing sufficient data of the minimum design measurements capable with the current equipment.

3.6.1 Microstructure Fabrication and Designs

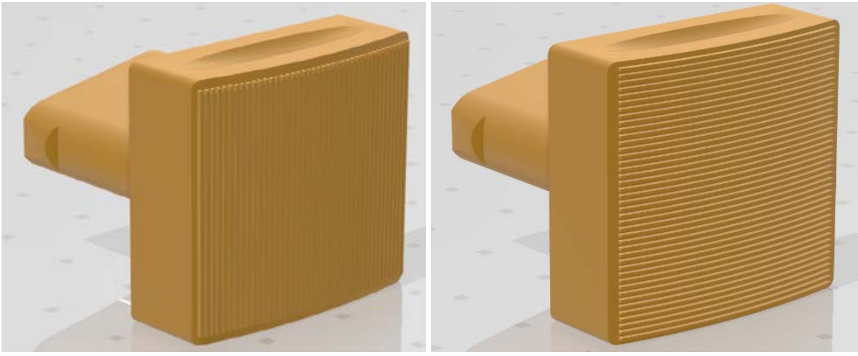

Figure 3-15: Parallel and Perpendicular Design

Figures 3-15, 3-16, 3-17, 3-18 are 3D images of the printed surfaces using the simplest linear designs. The parallel and perpendicular designs both share the same specifications.

- Line width:0.30mm or 300μm
- Line spacing:0.35mm 350μm
- Line length:25mm
- Total number of extrusions:39

The spacing was selected due to the printing limitations of the current equipment and results obtained from testing.

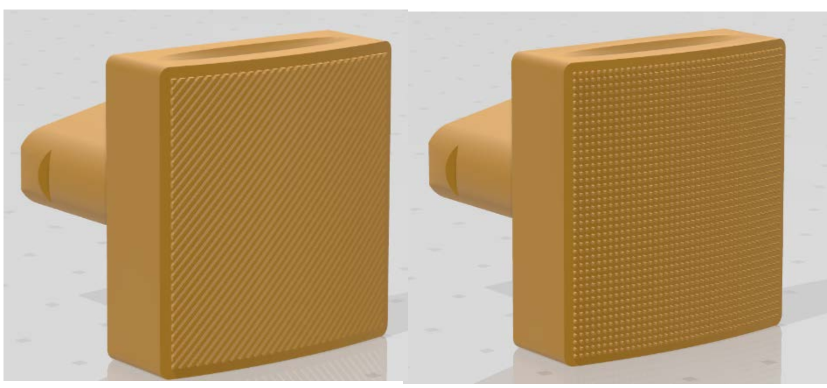

Figure 3-16: 45 degree and justified cylinder

The forty-five-degree design specifications are as follows:

- Line width: 0.30mm or 300μm
- Line spacing: 0.35mm or 350μm
- Line length: cut to fit 25mmx25mm
- Number of extrusions: 55

The justified cylinder design specifications are as follows:

- Cylinder diameter: 0.30mm or 300μm
- Spacing: 0.35mm or 350μm

- Number of extrusions:1444 (38x38)

The justified diamonds design specifications are as follows:

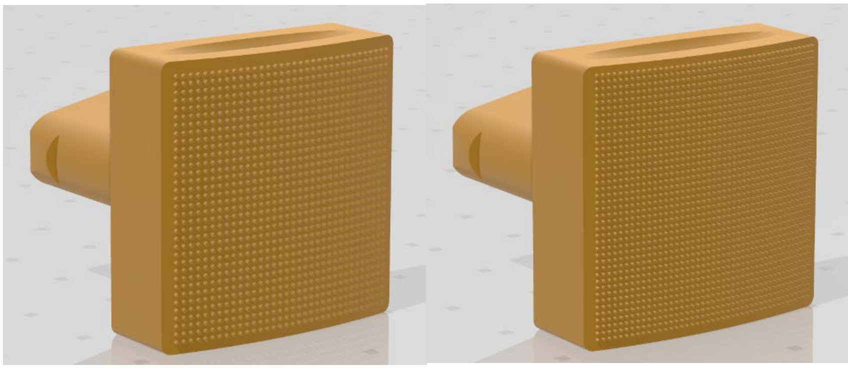

Figure 3-17: Justified diamond and hexagon

- Diamonds side length: 0.30mm or 300 µm
- Corner-to-corner length:0.42mm or 420 µm
- Spacing: 0.35mm or 350 µm
- Number of extrusions: 1024 (32x32)

The justified shark skin specifications are as follows:

- Line minimum length: 1.0mm
- Line length incremental increase: .50mm 500 µm
- Line max length: 3.0mm
- Line width: 0.30mm or 300 µm
- Line spacing vertically: 0.25mm or 250 µm
- Line spacing horizontally: 0.40mm or 400 µm

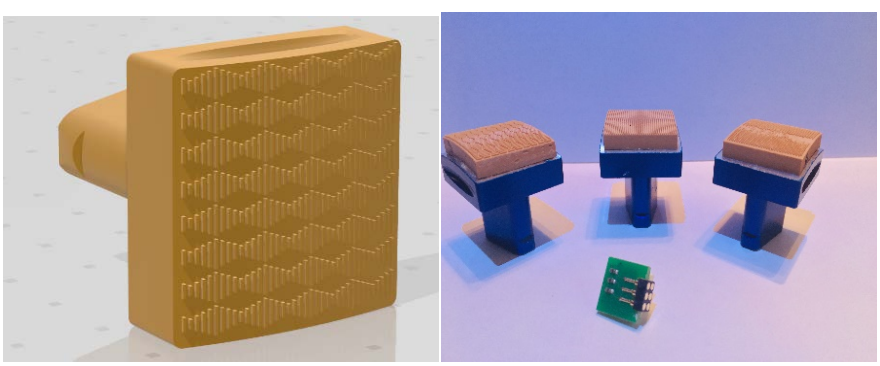

Figure 3-18: Justified shark skin design & assembled samples

Slight variations of these designs (justified & offset) will be created to determine if there is an impact on the measured DCOF. These changes will mainly be offsetting some designs to achieve more complex structures and removing excessive and unnecessary space. All extrusions were set to 0.5mm or 500 μm to reduce damage during testing. After statistical analysis, designs will be selected based on correlating data to human results for further investigation. Initial designs were printed and attached to metal inserts. This was selected versus printing the entire sensor due to print errors encountered and cost-saving means.

3.6.2 Ceramic-Polymer Tested Samples

Table 3-8 shows the obtained results of testing of three microstructure designs using a ceramic-polymer material on the same surfaces in the treatment study and the results obtained from a researcher walking across the surfaces on the variable angle ramp barefoot. These surfaces were polished porcelain, polished black granite, and textured glazed porcelain. The designs that were tested were parallel, shark skin, and cylinder designs. These results were then compared to the values obtained from the barefoot testing ton the ramp. It is important to note that the cylinder design experienced significant damage and breakage during testing on the textured glazed porcelain and could not be used on the polished black granite. Values obtained on the polished porcelain and textured glazed porcelain closely match the measured values of the designs on the same surface. However, values differ greatly on the polished black granite. Further research into this difference and its causes is necessary, but other results show promise. Additional designs and materials need to be tested as well to determine the connection between structures and materials

Table 3-8: Initial results with ceramic-polymer & barefoot comparison

Tile Type	Ramp DCOF values	Parallel design	Sharkskin design	Cylinder design
Polished Porcelain	.13	.15	.12	.12
Polished Black Granite	.16	.33	.31	N/A – Damaged
Textured Glazed Porcelain	.36	.38	.39	.43

Initial results showed promising results, however the large difference in the obtained polished black granite values in comparison to the barefoot values warranted a reconsideration of the material to be used. As mentioned earlier, a substitution was made to use a softer polymer in anticipation to more accurately represent plantar skin and reduce the difference.

3.7 Soft Polymer Testing

Using the same procedure as the ceramic-polymer, initial spacing tests were conducted in order to see what the minimum width and space between extrusions was necessary for a successful print.

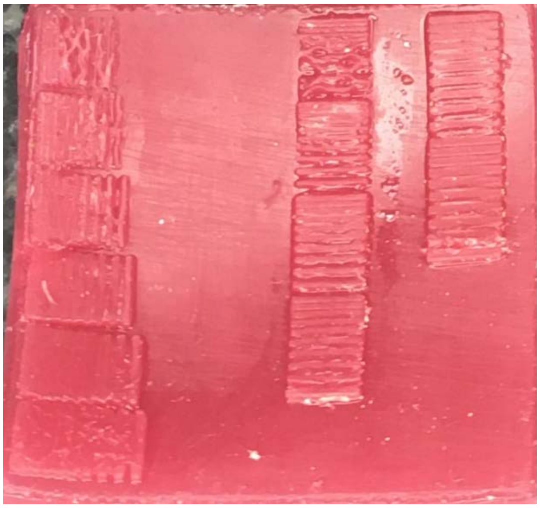

Figure 3-19: Soft polymer spacing test one

Using the same methodology as the ceramic-polymer, the spacing and line width used for the soft polymer yielded results that showed a wider space between extrusions was necessary for excess fluid to be drained between printing layers. Line widths >0.45 yielded little to no deformation but an increase between extrusions was necessary. Line width started at 0.1mm increasing by 0.05mm in the horizontal and vertical directions up to 0.35mm. Spacing started at 0.1mm increasing by 0.05mm up to 0.35mm.

Figure 3-20: Soft polymer spacing test two

Results pictured in Figure 3-19 and Figure 3-20 begin with a line width of 0.4mm up to 0.5mm in increments of 0.05mm. Spacing began at 0.3mm p to 0.7mm due to previous testing. The extrusion height in this example was set to 0.5mm. This test showed that a necessary wall thickness of 0.45mm was needed and a space of 0.7mm with an extrusion height of 0.5mm yielded desirable results.

3.7.1 Microstructure Fabrication and Design

This section will focus on the design utilizing the soft polymer material. The technical data provided by Envisiontec will be provided in Appendix A Technical specifications. The impact of the design on the DCOF will be a focus of this thesis along with a sufficient relationship to the barefoot testing will be made. The thickness of the base is approximately 2.5mm and approximately 25x25mm. The first designs will be the parallel and perpendicular lines.

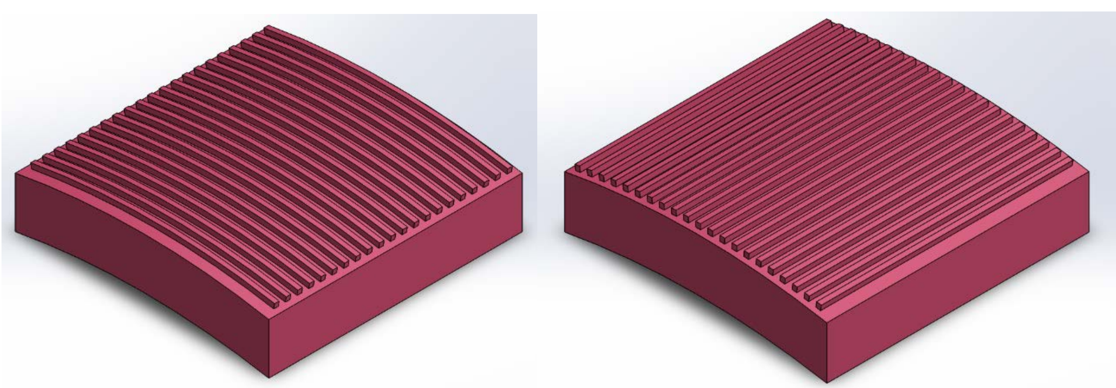

Figure 3-21: Parallel (left) and perpendicular (right) 3D model

The specifications for the following perpendicular and parallel designs are as follows:

- Number of extrusions: 21
- Extrusion height: 0.50mm
- Spacing between extrusions: 0.70mm

- Width of extrusions:0.45mm
- Length of extrusion: 24mm

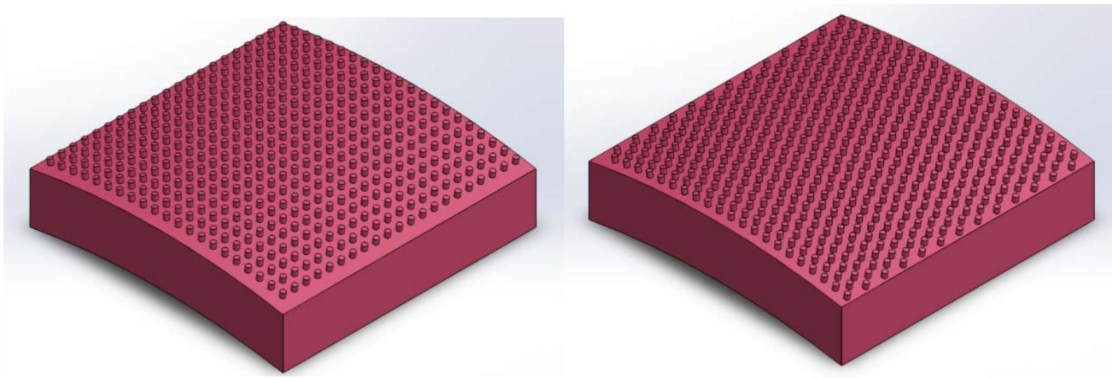

Figure 3-22: Justified (left) and offset (right) cylinder 3D model

The following specifications are for the justified cylinder designs:

- Number of extrusions: 441
- Extrusion height: 0.50mm
- Spacing between extrusions: 0.70mm
- Radius of cylinder: 0.225mm

The following specifications are for the offset cylinder design:

- Number of extrusions: 546
- Extrusion height: 0.50mm
- Spacing between extrusions: 0.70mm
- Radius of cylinders: 0.225mm

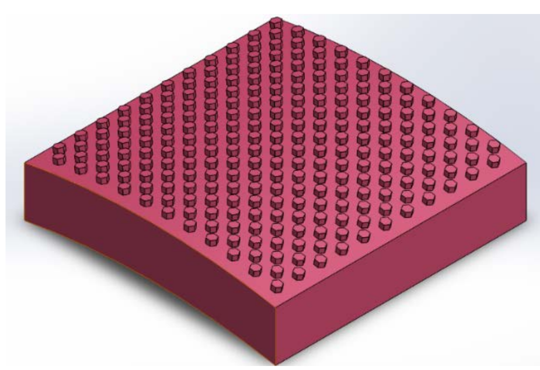

Figure 3-23: Offset hexagon 3D model

The following specifications are for the offset hexagon design:

- Number of extrusions: 242
- Extrusion height: 0.50mm
- Spacing between extrusions:
  - Horizontal space: 1.27mm
  - Vertical space: 1.38mm
  - Diagonal space: 0.7mm
- Width of extrusions: point-to-point – 0.90mm
- Length of extrusions: edge-to-edge – 0.78mm
- Side length: 0.45mm

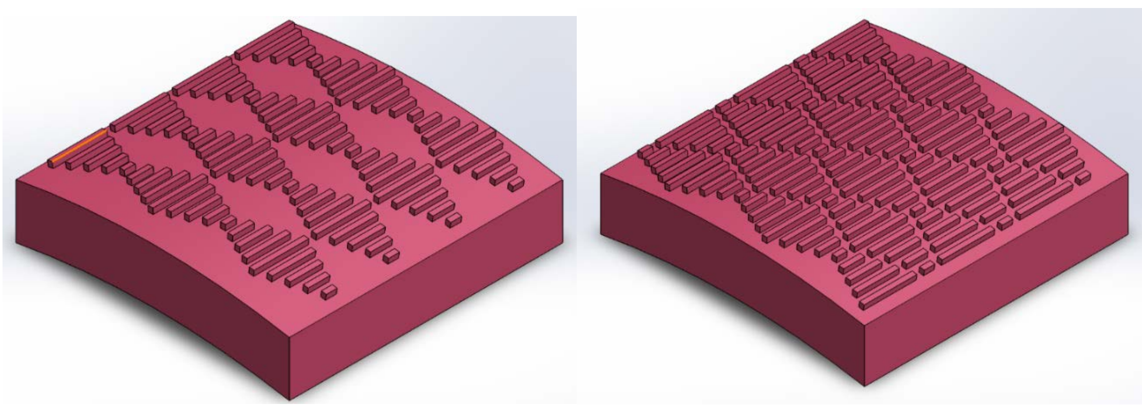

Figure 3-24: Justified (left) and offset (right) shark skin 3D model

The following specifications are for the justified shark skin design:

- Number of extrusions: 84
- Extrusions height: 0.50mm
- Spacing between extrusions:
- 0.70mm
- Width of extrusions: 0.45mm
- Length of extrusions: begins at 5.0mm down to 1.0mm in increments of 1.0mm

The following specifications are for the offset shark skin design:

- Number of extrusions: 126
- Extrusions height: 0.50mm
- Spacing between extrusions: 0.7mm
- Width of extrusions: 0.45mm
- Length of extrusions: begins at 5.0mm down to 1.0mm in increments of 1.0mm

The sharkskin designs were rotated so additional designs include parallel and perpendicular designs as well as offset and justified.

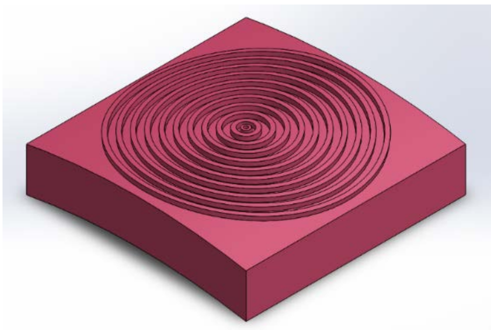

Figure 3-25: Concentric circle 3D model

The following specifications are for the concentric circle design:

- Number of extrusions: 11
- Extrusion height: 0.50mm
- Spacing between extrusions: 0.7mm
- Width of extrusions:0.45mm

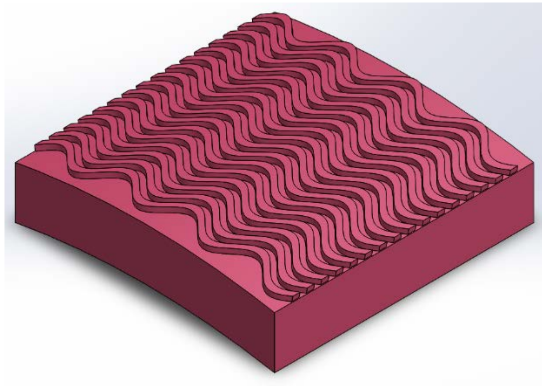

Figure 3-26: Sine wave 3D model

The following specifications are for the sine wave design:

- Number of extrusions: 16
- Extrusion height: 0.50mm
- Spacing between extrusions: ~0.7mm
- Width of extrusions: ~0.45mm
- Length of extrusions: ~25mm

The parameters obtained from the spacing test were used as the foundation for all the designs shown. The shark skin, hexagons, diamonds, and cylinders are all based on biomimetic designs discussed in the paper written by Malshe et al. The parallel, perpendicular, concentric circles, and sine wave were all used to try to simplify the natural ridges that occur on human skin. A solid soft polymer sample will be used as a reference in order to compare any possible differences between the designs. But it important to note that the purpose is not to copy the microstructure of human skin, but to instead replicate the frictional properties of human skin.

3.7.2 Biomimetic and Barefoot Data

This section includes the data collected during the testing of the biomimetic surface and the values obtained from the barefoot testing done. The biomimetic surfaces were tested. Designs were tested on the same surfaces as the variable angle ramp, the lubricant used was 10W-30 SAE oil. Enough oil was applied to the surface to ensure the sensor would remain in the lubricant throughout the ten-inch measurement. It is important to note that since not all of the entire 25mmx25mm and only a small portion of the sensor comes into contact with the sample surfaces an entire design is not necessary. In order to save material and reduce costs, this was applied for some of the more complex designs. Many of the designs tested tended to cluster around the same values despite changes in the surface. Furthermore, only travertine and textured glazed porcelain surfaces showed any large differences from the mean values of each design. From comparing values obtained from testing the sensor to results obtained from the variable angle ramp, three designs produced results similar. These designs are parallel sine waves, perpendicular lines, and a solid sensor with no design. Statistical analysis of the all designs will be done along with a Tukey pairwise comparison at the 95% confidence level for the three mentioned designs and the barefoot data values. This will be done in order to see if the designs are statistically discernable from the barefoot values or if they are considered to be statistically the same in their results. This is an important step into establishing a relationship between experimental designs and actual measurements of human skin utilizing a standardized testing method that is widely accepted and extensively tested. All tests were carried out in the same day under the same experimental conditions. The temperature of the room was ~23°C ± 3°C with a relative humidity of ~45% ± 3%.

Table 3-9: Biomimetic DCOF testing

	Concentric Circles	Justified cylinder	Offset cylinders	Offset hexagons	Para. lines	Perp. lines	Solid	Perp. offset sharkskin	Para. justified sharkskin	Perp. sine wave	Para. sine wave
Beige Ceramic	0.19	0.13	0.13	0.13	0.18	0.07	0.09	0.12	0.11	0.13	0.07
Polished black granite	0.17	0.13	0.11	0.12	0.19	0.06	0.09	0.13	0.11	0.12	0.07
White viena ceramic	0.18	0.12	0.11	0.12	0.17	0.06	0.09	0.12	0.11	0.12	0.07
Polished white marble	0.17	0.13	0.12	0.13	0.17	0.08	0.09	0.14	0.13	0.14	0.08
Travertine	0.26	0.22	0.22	0.21	0.37	0.13	0.12	0.23	0.19	0.2	0.14
Polished porcelain	0.17	0.13	0.12	0.13	0.2	0.05	0.09	0.13	0.12	0.12	0.06
Textured glazed porcelain	0.35	0.31	0.32	0.31	0.38	0.2	0.28	0.34	0.26	0.27	0.21
Polished white porcelain	0.17	0.13	0.12	0.13	0.29	0.05	0.09	0.13	0.12	0.12	0.06
Slate ceramic	0.51	0.48	0.52	0.51	0.57	0.41	0.45	0.54	0.44	0.48	0.43

Table 3-10: Variable angle ramp barefoot values

	Test 1	Test 2	Test 3	Average	DCOF
Test subject 1					
Standard surface 1	9.5	8.1	8.5	8.70	0.15
Standard surface 2	20	21.9	20.4	20.77	0.38
Standard surface 3	26.3	27.1	27.1	26.83	0.51
Beige ceramic	3.4	4.3	3.8	3.83	0.07
Polished black granite	4.3	3.1	3	3.47	0.06
White viena ceramic	3.9	3.5	4.7	4.03	0.07
Polished white marble	3.6	3.5	3	3.37	0.06
Travertine	2.3	3.4	3.9	3.20	0.06
Polished porcelain	2.7	2.6	2.3	2.53	0.04
Textured glazed porcelain	2.8	5	4.6	4.13	0.07
Polished white porcelain	2.2	3.6	3.4	3.07	0.05
Slate ceramic	3.3	3.4	3.8	3.50	0.06
Test subject 2					

	Test 1	Test 2	Test 3	Average	DCOF
Test subject 1					
Standard surface 1	8.8	10.5	11.5	10.27	0.18
Standard surface 2	18.7	17	17.8	17.83	0.32
Standard surface 3	25	27.9	28.7	27.20	0.51
Beige ceramic	3.2	2.9	2.6	2.90	0.05
Polished black granite	2.6	3.1	4.1	3.27	0.06
White viena ceramic	3.3	4.5	3.1	3.63	0.06
Polished white marble	2.3	2.3	2	2.20	0.03
Travertine	3.4	2.1	2.7	2.73	0.05
Polished porcelain	2.8	2.7	2.6	2.7	0.05
Textured glazed porcelain	4.2	3.7	4	3.97	0.07
Polished white porcelain	3	3.9	3.3	3.4	0.06
Slate ceramic	3.5	2.4	4.2	3.37	0.06

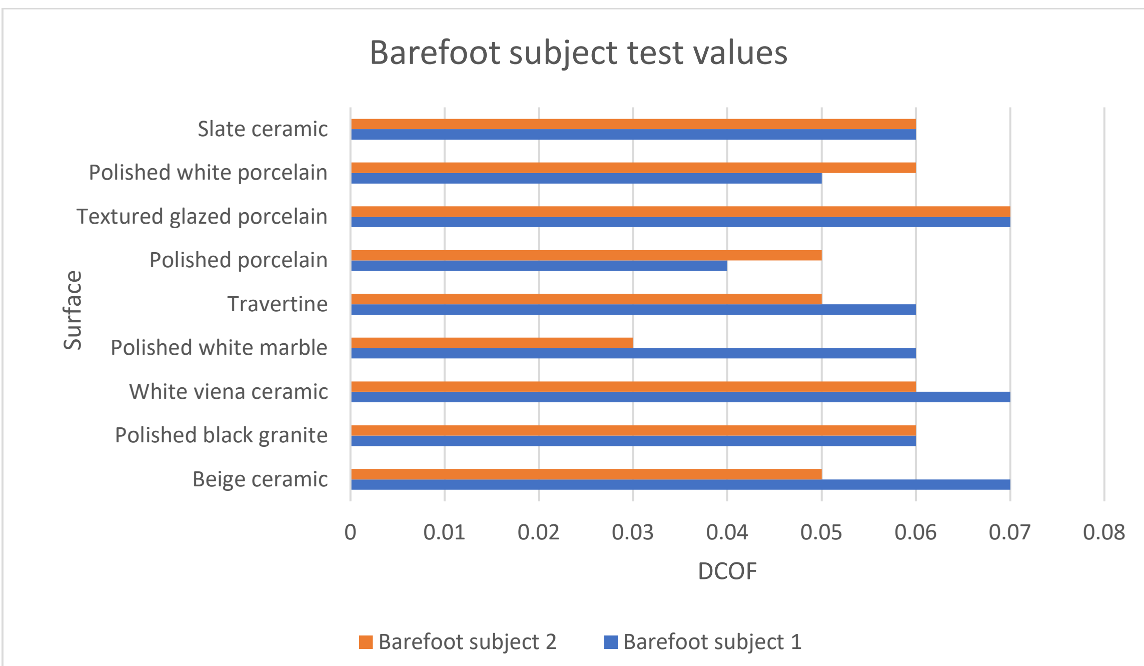

Figure 3-27: Barefoot subject values on a line graph

Values obtained from the barefoot testing show extraordinarily low DCOF values while subjects walked across the surfaces barefoot through 10W-30 SAE oil. Some biomimetic designs did measure near the values obtained from human testing.

Statistical analysis and comparisons of the measured DCOF values will be in the following section. Additionally, statistical analysis over the treatment study values and methods will be done as well.

CHAPTER 4

STATISTICAL ANALYSIS

The statistical analysis for the treatment study and the soft polymer designs will be covered in the following section. Statistical analysis is important and used to determine whether or not factors can be considered significantly different in the impact they may or may not have on the response variable. For the analysis, Minitab will be utilized. The analysis of variance provides a tough and impartial method for making inferences about the behavior of the modeled data. ANOVA infers that the variation in the modeled data collected can be divided in a way that an approximation of the contributions of factors and the degree to which they affect the response variable. An experiment-wise error rate of $\alpha = 0.05$ will be used. This is the level of statistical significance. Should the calculated P-value be < 0.05 then the factor is said to be statistically discernable in the impact it has on the response variable.

4.1 Treatment Statistical Analysis

The analysis of variance for the treatment study will consider the factors of testing method, treatment application, and surface have on the response variable – DCOF. The different types of methods are:

1. Drag sled
2. Variable angle ramp
3. Pendulum

The names of the treatments have been replaced as treatments A, B, C, D, E, and untreated. Samples were left untreated to view any changes that may have occurred from the application of the treatment. The surfaces tested on were polished porcelain, polished black granite, and textured glazed porcelain.

Table 4-1: ANOVA DCOF versus method, treatment, and surface

General Linear Model: DCOF versus Method, Treatment, Surface

Method

Factor coding (-1, 0, +1)

Factor Information

Factor	Type	Levels	Values
Method	Fixed	3	1 – drag sled, 2 – variable angle ramp, 3 - pendulum
Treatment	Fixed	6	1 - untreated, 2 - A, 3 - B, 4 - C, 5- D, 6 - E
Surface	Fixed	3	1 – polished porcelain, 2 – polished black granite, 3 – textured glazed porcelain

Analysis of Variance

Source	DF	Adj SS	Adj MS	F-Value	P-Value
Method	2	0.38723	0.193617	46.73	0.000
Treatment	5	0.34682	0.069363	16.74	0.000
Surface	2	1.27390	0.636950	153.73	0.000
Method*Treatment	10	0.11143	0.011143	2.69	0.029
Method*Surface	4	0.11907	0.029767	7.18	0.001
Treatment*Surface	10	0.36157	0.036157	8.73	0.000
Error	20	0.08287	0.004143		
Total	53	2.68288			

Model Summary

S	R-sq	R-sq(adj)	R-sq(pred)
0.0643687	96.91%	91.81%	77.48%

Coefficients

Term	Coef	SE Coef	T-Value	P-Value	VIF
Constant	0.41722	0.00876	47.63	0.000	
Method					
1	-0.0522	0.0124	-4.22	0.000	1.33
2	0.1194	0.0124	9.64	0.000	1.33
Treatment					
1	-0.1006	0.0196	-5.13	0.000	1.67
2	-0.1083	0.0196	-5.53	0.000	1.67
3	0.1061	0.0196	5.42	0.000	1.67
4	0.0450	0.0196	2.30	0.033	1.67
5	0.0583	0.0196	2.98	0.007	1.67
Surface					
1	-0.0950	0.0124	-7.67	0.000	1.33
2	-0.1217	0.0124	-9.82	0.000	1.33
Method*Treatment					
1 1	0.0322	0.0277	1.16	0.258	2.22
1 2	-0.0500	0.0277	-1.81	0.086	2.22
1 3	0.0222	0.0277	0.80	0.432	2.22
1 4	-0.0200	0.0277	-0.72	0.479	2.22
1 5	-0.0200	0.0277	-0.72	0.479	2.22

2 1	-0.0761	0.0277	-2.75	0.012	2.22
2 2	-0.0183	0.0277	-0.66	0.516	2.22
2 3	-0.0161	0.0277	-0.58	0.567	2.22
2 4	0.0817	0.0277	2.95	0.008	2.22
2 5	0.0650	0.0277	2.35	0.029	2.22
Method*Surface					
1 1	0.0233	0.0175	1.33	0.198	1.78
1 2	0.0667	0.0175	3.81	0.001	1.78
2 1	-0.0083	0.0175	-0.48	0.639	1.78
2 2	-0.0283	0.0175	-1.62	0.121	1.78
Treatment*Surface					
1 1	-0.0250	0.0277	-0.90	0.378	2.22
1 2	0.0517	0.0277	1.87	0.077	2.22
2 1	0.0094	0.0277	0.34	0.737	2.22
2 2	0.1694	0.0277	6.12	0.000	2.22
3 1	0.0983	0.0277	3.55	0.002	2.22
3 2	-0.1217	0.0277	-4.39	0.000	2.22
4 1	0.0061	0.0277	0.22	0.828	2.22
4 2	-0.0372	0.0277	-1.34	0.194	2.22
5 1	0.0161	0.0277	0.58	0.567	2.22
5 2	-0.0606	0.0277	-2.19	0.041	2.22

Fits and Diagnostics for Unusual Observations

Obs	DCOF	Fit	Resid	Std Resid	
40	0.2400	0.1544	0.0856	2.18	R

R Large residual

From Table 4-1, it can be seen that the method, treatment, surface, and the interaction between these factors are statistically discernable in the impact they have on the measured values. This can be evident by comparing the calculated P-values of the factors and the level of confidence of 0.05 where all calculated values fall below the level of confidence set at the beginning of the analysis. The level of interaction between the factors was limited to two-way interactions and the three-way interaction was attributed to the error for the calculations. Since all factors were fixed we can conclude that not all the level means are equal. Because the interactions were also significant, we can conclude that this is dependent on the other factors in the related term. Examining the residual plots provides insight into whether the model is satisfactory and meets all the expectations made at the beginning of the analysis. The normal probability plot shows the residuals forming a very linear line. There does not appear to be any signs of unnamed variables or lack of normality in the plot. However, there was an indicated measurement that had a large residual. Investigation into the details of this measurement is warranted. The residual versus order plot can be used to confirm that there does not appear to be any obvious trends or patterns. The values appear to randomly fall about the centerline and no immediate evidence to assume the residuals are not independent. Residual plots of the measured data were created versus the method, surface, and treatment. No obvious trends were detected.

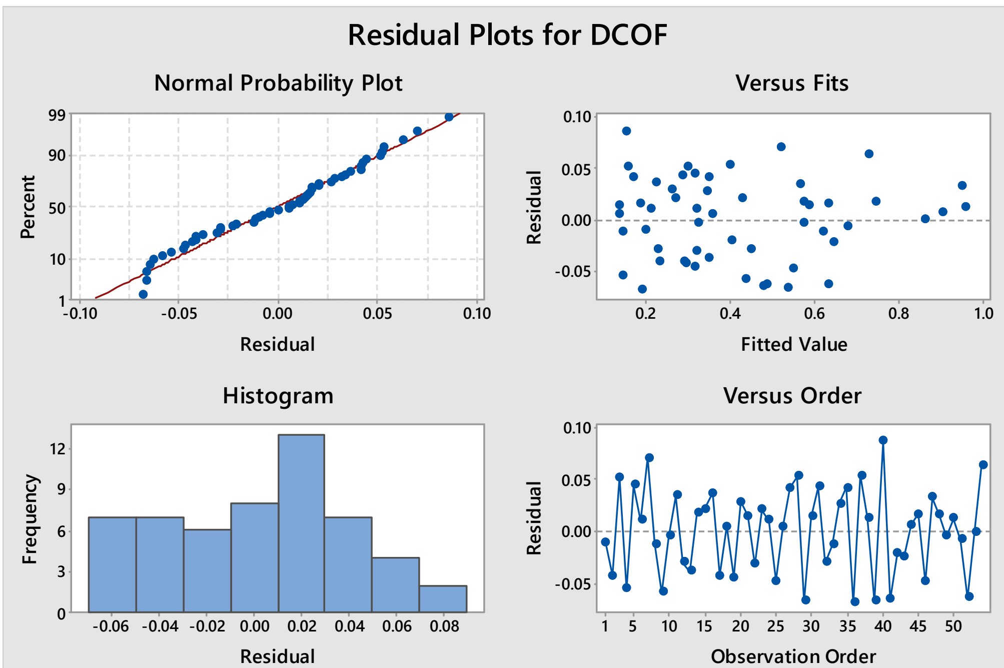

Figure 4-1: Residual plots

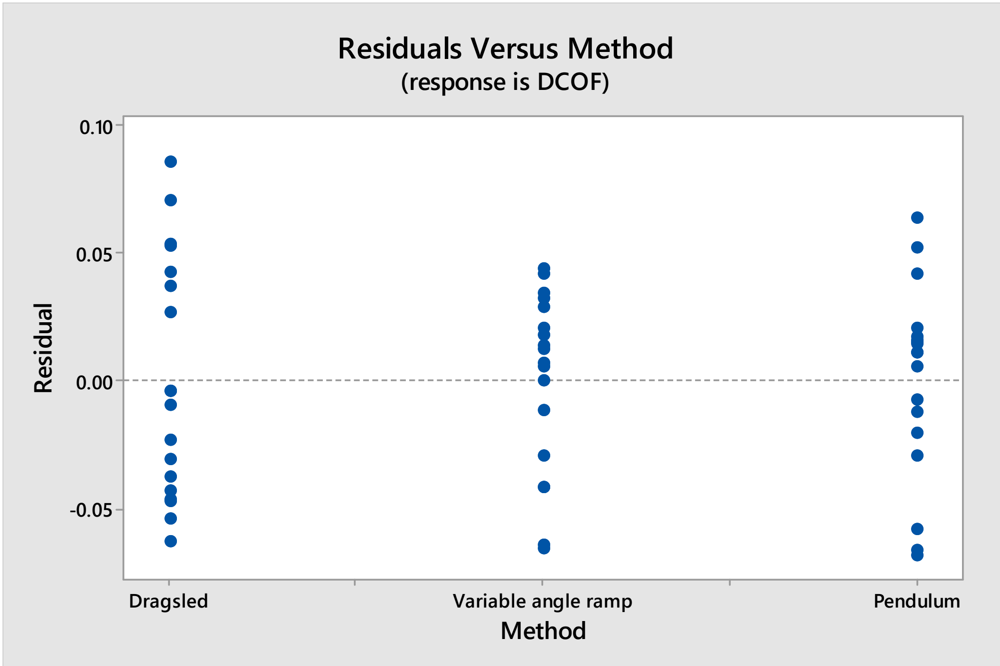

Figure 4-2: Residual versus method

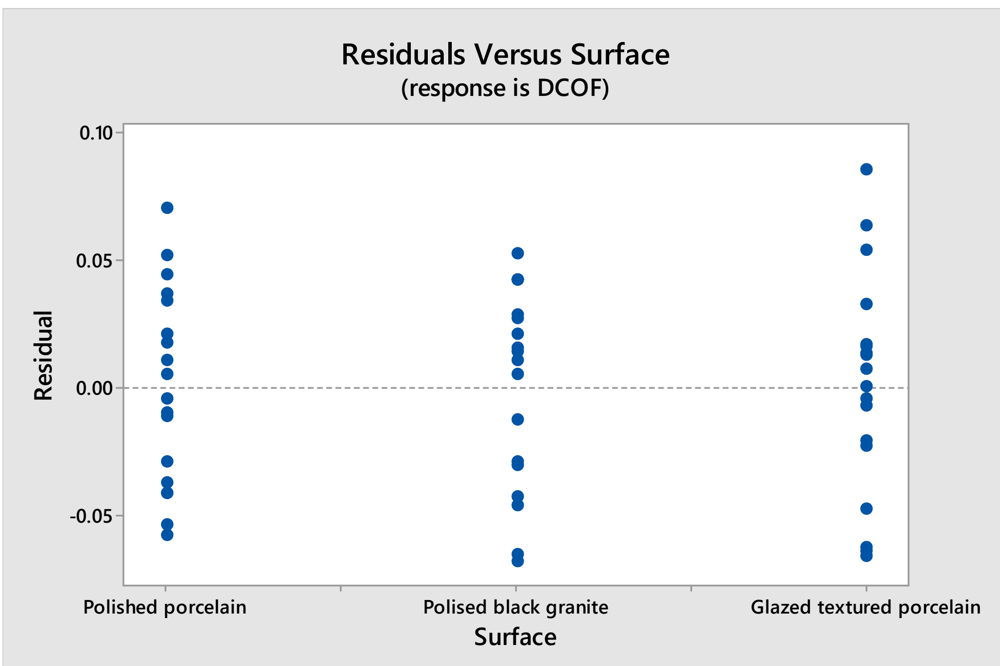

Figure 4-3: Residual versus surface

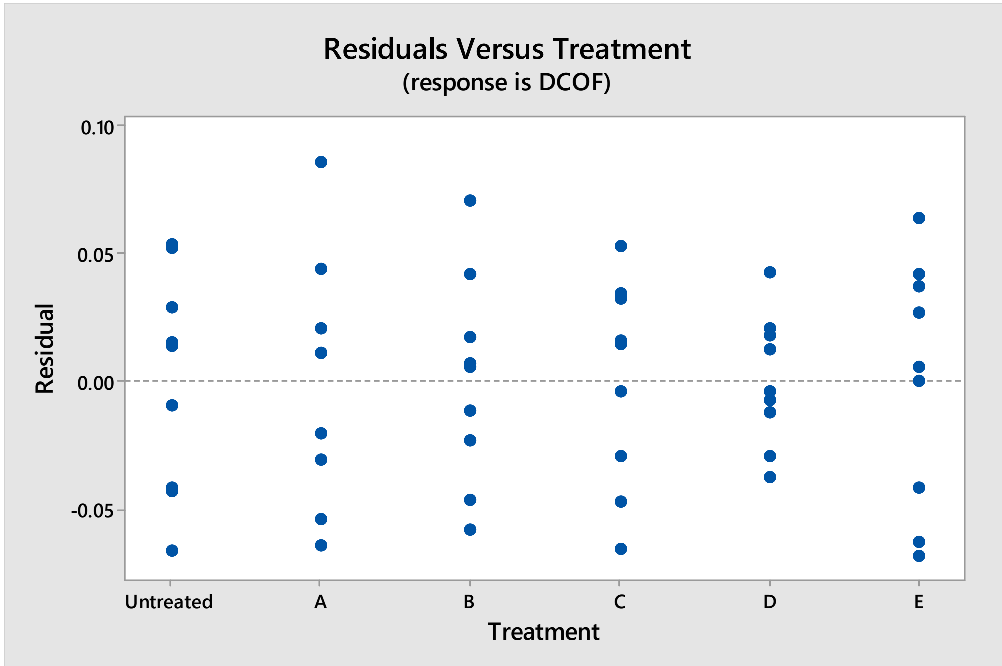

Figure 4-4: Residual versus treatments

Boxplots of the data versus the surface, method, and treatments were created. This allows us to graphically analyze the data and look for differences and similarities between the data under different circumstances. Looking at Figure 4-5 we can see that the average of the polished porcelain and polished black granite fall near each other. While the textured porcelain appears higher in DCOF with a wider range than the other two types of surface. Analyzing Figure 4-6 shows that the variable angle ramp method on average had higher numbers than the other two methods while the drag sled and pendulum averages appear to be very close together. The variable angle ramp and pendulum data appears to have a larger range than the drag sled method. The pendulum data appears to be skewed to the right with majority of the data appearing on the lower side of the DCOF measurements. Finally, Figure 4-7 shows the box plot for the treatment DCOF. As expected the untreated DCOF mean values are very low. While the ranges on most of the other treatments cover a large difference, the mean value for three of the treatments appear to be very similar to one another. Product B's mean DCOF appears to be higher than other treatments. Figure 4-8 shows an interaction plot of the different factors. When analyzing an interaction plot the more nonparallel lines there are the greater the interaction is between the factors. The highest obtained values in the method*surface interaction was between the variable angle ramp and the textured glazed porcelain, and between the method*treatments the highest obtained values were between the interactions of treatments B, C, and D using the variable angle ramp. The textured glazed porcelain seemed to be the most responsive to the different types of treatments in raising the DCOF values. The variable angle ramp appears to show the highest DCOF values for the treatments. Treatments B-E seemed to be most applicable on the textured glazed porcelain. From Figure 4-9 the main effects plot we can note that between the methods, treatments, and surfaces there is a main outcome present and the response variable is not the same across all factor levels in this study. The steeper the slope of the line between points the greater the magnitude of the main effect. From the general linear model analysis of variance, we determined that there is a statistically discernible effect of the treatment, method, surface, and the interaction between these factors. It is also worth noting that the average mean value for DCOF approximately 0.42 with treatments B, C, D coming in above this value.

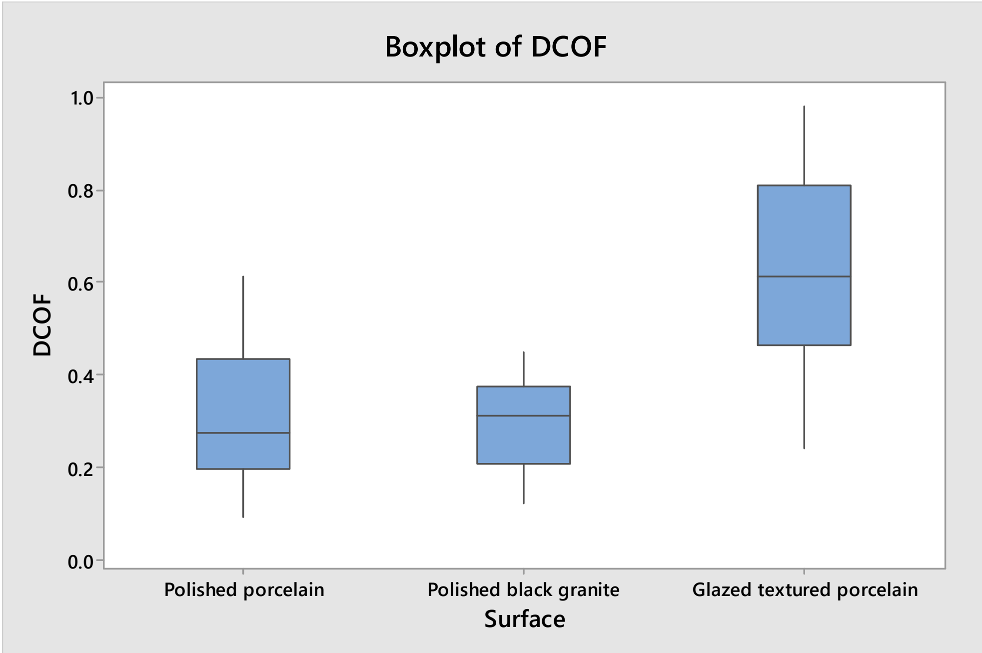

Figure 4-5:Surface boxplot

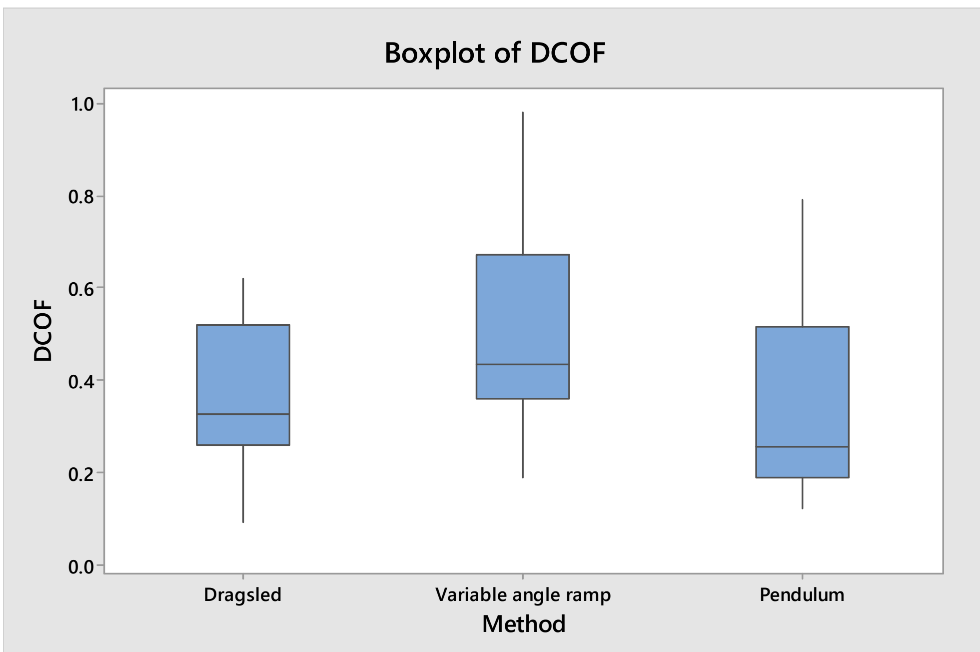

Figure 4-6: Method boxplot

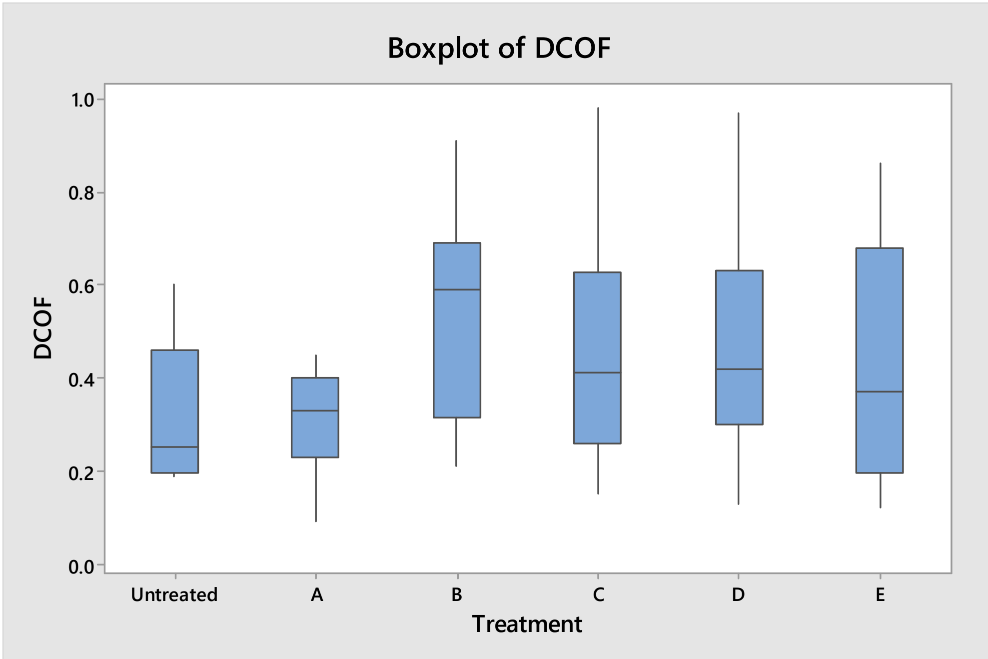

Figure 4-7: Treatment boxplot

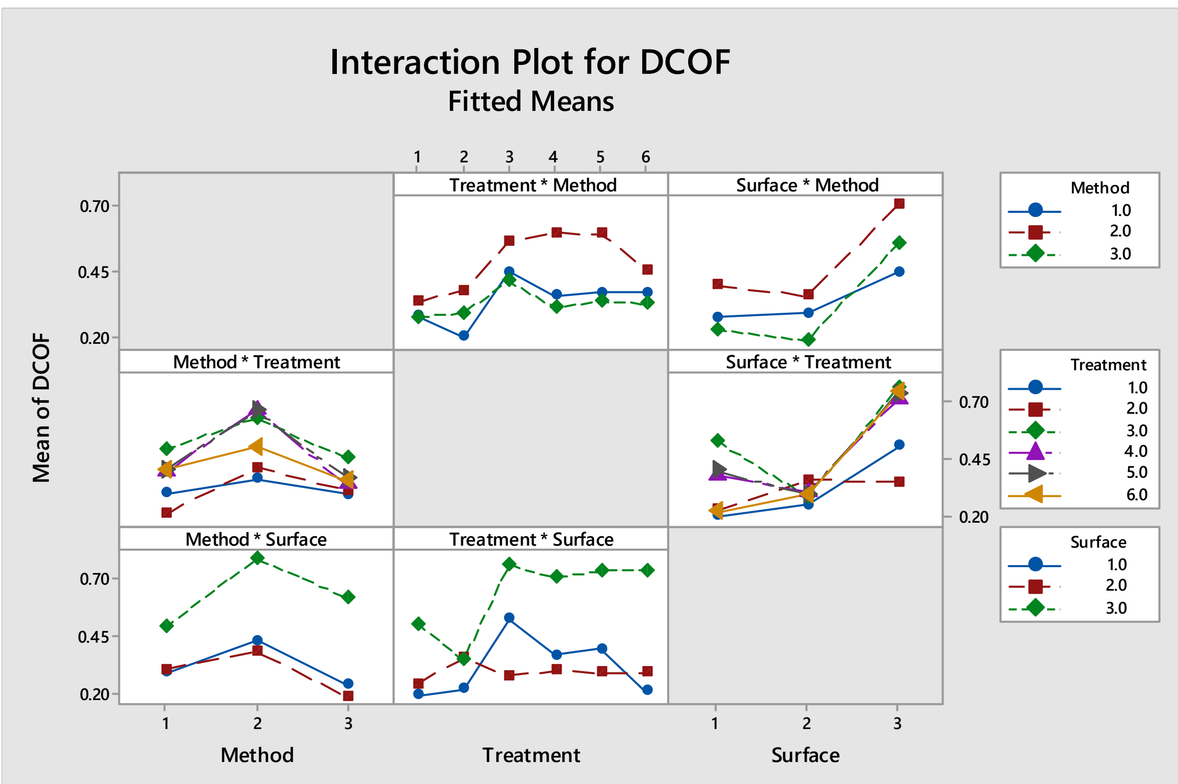

Figure 4-8: Interaction plots

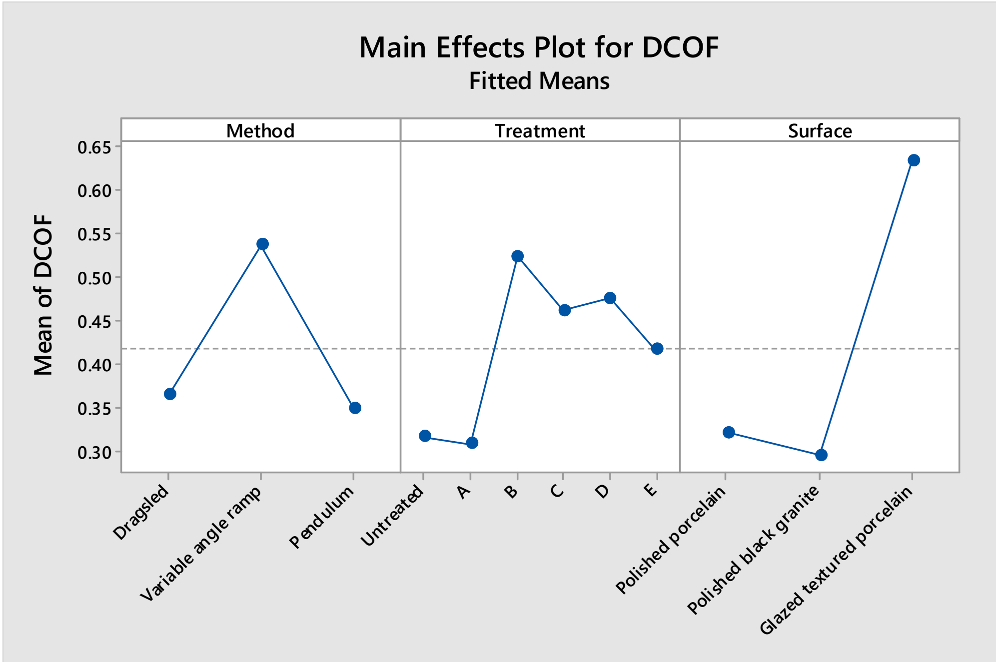

Figure 4-9: Main effects plot

Fisher least significant difference was used to compare the different levels within each factor. The variable angle ramp was determined to be statistically discernable from the other two methods. Treatment A and the untreated samples were shown to be statistically discernable from the rest of the treatments. The textured glazed porcelain was also shown to be statistically discernable from the other surfaces as well. Untreated surfaces were labeled as 1, treatment A is labeled as 2, B is labeled as 3, and so on up to treatment E being 6. From the fisher pairwise test in Table 4-2 provided it can be shown that the drag sled and variable angle ramp are not statistically discernable from one another while the pendulum is. The textured glazed ceramic is also shown to be statistically discernable from the rest of the other surfaces used in this study. Finally, treatments B and D were shown to be statistically discernable from the rest of the treatments and untreated samples.

Table 4-2: Fisher pairwise comparison of treatment DCOFs versus method, surface, and treatment

Comparisons for Treatment dcofs

Fisher Pairwise Comparisons: Method

Grouping Information Using Fisher LSD Method and 95% Confidence

Method	N	Mean	Grouping	
3 – Pendulum	24	0.498750	A	
1 – Drag sled	24	0.342500		B
2 – Variable angle ramp	24	0.314583		B

Means that do not share a letter are significantly different.

Fisher Individual Tests for Differences of Means

Difference of Method Levels	Difference of Means	SE of Difference	Individual 95% CI	T-Value	P-Value
2 - 1	-0.0279	0.0454	(-0.1187, 0.0628)	-0.62	0.541
3 - 1	0.1562	0.0454	(0.0655, 0.2470)	3.44	0.001
3 - 2	0.1842	0.0454	(0.0934, 0.2749)	4.06	0.000

Simultaneous confidence level = 87.91%

Fisher Pairwise Comparisons: Surfaces

Grouping Information Using Fisher LSD Method and 95% Confidence

Surfaces	N	Mean	Grouping	
4 – Textured glazed ceramic	18	0.633889	A	
1 – Polished porcelain	18	0.321111		B
3 – VCT	18	0.293889		B
2 – Polished black granite	18	0.292222		B

Means that do not share a letter are significantly different.

Fisher Individual Tests for Differences of Means

Difference of Surfaces Levels	Difference of Means	SE of Difference	Individual 95% CI	T-Value	P-Value
2 – 1	-0.0289	0.0524	(-0.1337, 0.0759)	-0.55	0.584
3 - 1	-0.0272	0.0524	(-0.1320, 0.0776)	-0.52	0.605
4 - 1	0.3128	0.0524	(0.2080, 0.4176)	5.97	0.000
3 - 2	0.0017	0.0524	(-0.1031, 0.1065)	0.03	0.975
4 - 2	0.3417	0.0524	(0.2369, 0.4465)	6.52	0.000
4 - 3	0.3400	0.0524	(0.2352, 0.4448)	6.49	0.000

Simultaneous confidence level = 80.06%

Fisher Pairwise Comparisons: Treatment

Grouping Information Using Fisher LSD Method and 95% Confidence

Treatment	N	Mean	Grouping
3 – B	12	0.518333	A
5 – D	12	0.500833	A

1 – Untreated	12	0.349167	B
4 – C	12	0.345833	B
6 – E	12	0.312500	B
2 – A	12	0.285000	B

Means that do not share a letter are significantly different.

Fisher Individual Tests for Differences of Means

Difference of Treatment Levels	Difference of Means	SE of Difference	Individual 95% CI	T-Value	P-Value
2 - 1	-0.0642	0.0642	(-0.1925, 0.0642)	-1.00	0.321
3 - 1	0.1692	0.0642	(0.0408, 0.2975)	2.64	0.011
4 - 1	-0.0033	0.0642	(-0.1317, 0.1250)	-0.05	0.959
5 - 1	0.1517	0.0642	(0.0233, 0.2800)	2.36	0.021
6 - 1	-0.0367	0.0642	(-0.1650, 0.0917)	-0.57	0.570
3 - 2	0.2333	0.0642	(0.1050, 0.3617)	3.64	0.001
4 - 2	0.0608	0.0642	(-0.0675, 0.1892)	0.95	0.347
5 - 2	0.2158	0.0642	(0.0875, 0.3442)	3.36	0.001
6 - 2	0.0275	0.0642	(-0.1009, 0.1559)	0.43	0.670
4 - 3	-0.1725	0.0642	(-0.3009, -0.0441)	-2.69	0.009
5 - 3	-0.0175	0.0642	(-0.1459, 0.1109)	-0.27	0.786
6 - 3	-0.2058	0.0642	(-0.3342, -0.0775)	-3.21	0.002
5 - 4	0.1550	0.0642	(0.0266, 0.2834)	2.41	0.019
6 - 4	-0.0333	0.0642	(-0.1617, 0.0950)	-0.52	0.605
6 - 5	-0.1883	0.0642	(-0.3167, -0.0600)	-2.93	0.005

Simultaneous confidence level = 64.55%

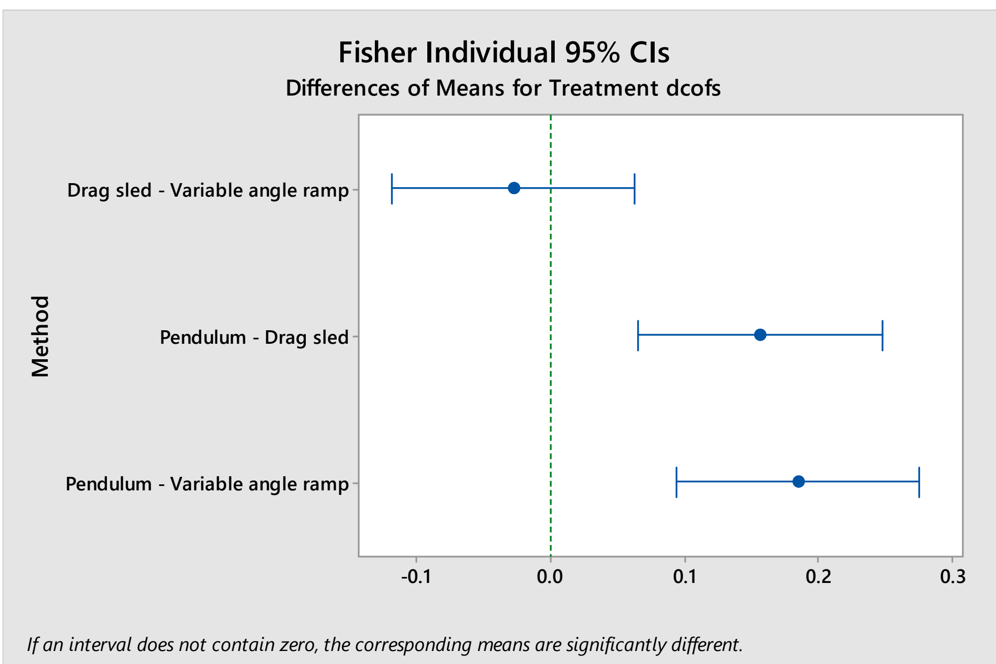

Figure 4-10: Fisher pairwise graph of method intervals

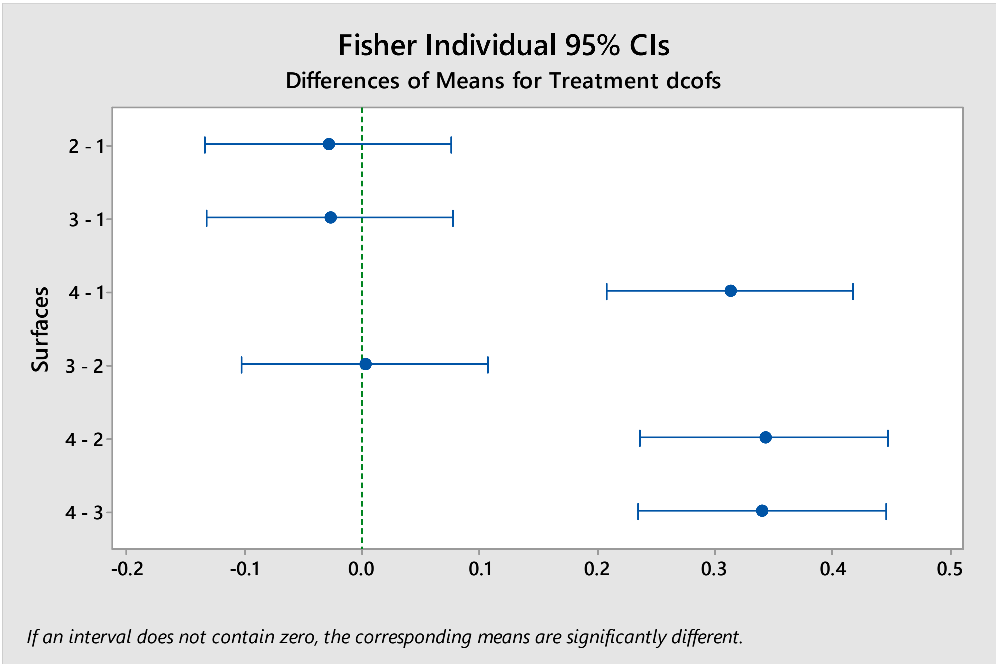

Figure 4-11: Fisher pairwise graph of surface intervals

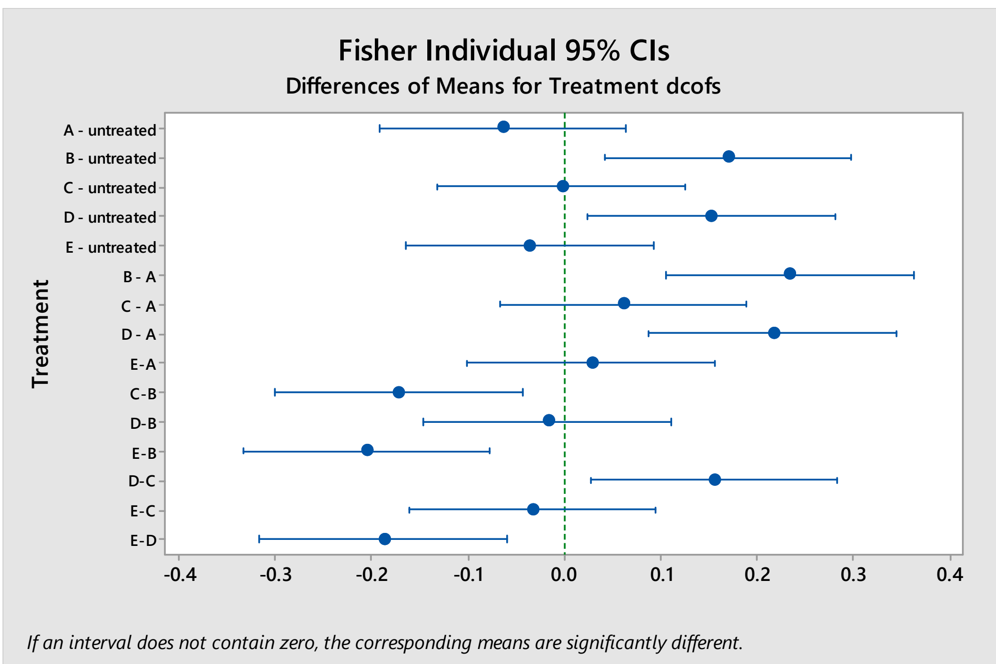

Figure 4-12: Fisher pairwise graph of treatment intervals

The fisher pairwise interval graphs support the same findings that were found within the calculated data provided in Table 4-2.

4.2 Soft Polymer Statistical Analysis

An analysis of the variance using a fit general linear model was used to determine the effects of the designs on the measured values. A comparison of the different designs to the barefoot values will be used as well. This will be done at a level of confidence of ninety-five. The following information was obtained.

Table 4-3: Biomimetic DCOF versus design and surface

General Linear Model: B.DCOF versus Design, Surface

Method

Factor coding (-1, 0, +1)

Factor Information

Factor	Type	Levels	Values
Design	Fixed	13	1, 2, 3, 4, 5, 6, 7, 8, 9, 10, 11, 12, 13
Surface	Fixed	9	1, 2, 3, 4, 5, 6, 7, 8, 9

Analysis of Variance

Source	DF	Adj SS	Adj MS	F-Value	P-Value
Design	12	0.4562	0.038015	15.34	0.000
Surface	8	1.1874	0.148419	59.88	0.000
Error	96	0.2380	0.002479		
Total	116	1.8815			

Model Summary

S	R-sq	R-sq(adj)	R-sq(pred)
0.0497868	87.35%	84.72%	81.21%

Coefficients

Term	Coef	SE Coef	T-Value	P-Value	VIF
Constant	0.17026	0.00460	36.99	0.000	
Design					
1 – concentric circles	0.0709	0.0159	4.44	0.000	1.85
2 – justified cylinders	0.0275	0.0159	1.73	0.088	1.85
3 – offset cylinders	0.0264	0.0159	1.66	0.101	1.85
4 – offset hexagons	0.0286	0.0159	1.80	0.076	1.85
5 – parallel lines	0.1097	0.0159	6.88	0.000	1.85
6 – perpendicular lines	-0.0469	0.0159	-2.94	0.004	1.85
7 – solid with no design	-0.0158	0.0159	-0.99	0.324	1.85
8 – perpendicular offset shark skin	0.0386	0.0159	2.42	0.017	1.85
9 – parallel justified shark skin	0.0064	0.0159	0.40	0.689	1.85
10 – perpendicular sine waves	0.0186	0.0159	1.17	0.245	1.85
11 – parallel sine waves	-0.0380	0.0159	-2.39	0.019	1.85
12 – barefoot test subject 1	-0.1103	0.0159	-6.92	0.000	1.85
Surface					
1	-0.0572	0.0130	-4.39	0.000	1.78
2	-0.0610	0.0130	-4.69	0.000	1.78
3	-0.0626	0.0130	-4.81	0.000	1.78

4	-0.0572	0.0130	-4.39	0.000	1.78
5	0.0144	0.0130	1.10	0.273	1.78
6	-0.0618	0.0130	-4.75	0.000	1.78
7	0.0890	0.0130	6.83	0.000	1.78
8	-0.0533	0.0130	-4.10	0.000	1.78

Fits and Diagnostics for Unusual Observations

Obs	B.DCOF	Fit	Resid	Std Resid	
108	0.0600	0.3097	-0.2497	-5.54	R
117	0.0600	0.3042	-0.2442	-5.41	R

R Large residual

The design and surfaces were both determined to be statistically discernable in the effect they have on the measurable DCOF. A review of the residuals for the statistical analysis shows a near linear fit on the normal probability plot and two measurements that have a large residual in the fit and order plots. An R-sq value of 87.35% was obtained as well. Some large residuals were detected and outline within the statistical analysis and is visible in Figure 4-14. These were both present on surface nine the slate ceramic samples.

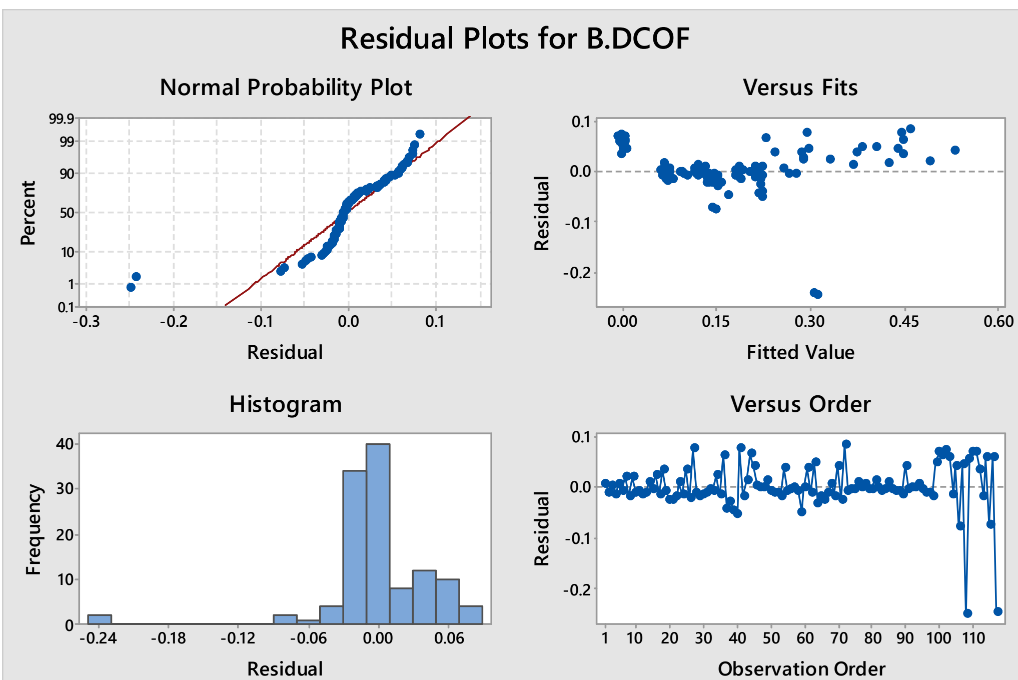

Figure 4-13: Design residual plots

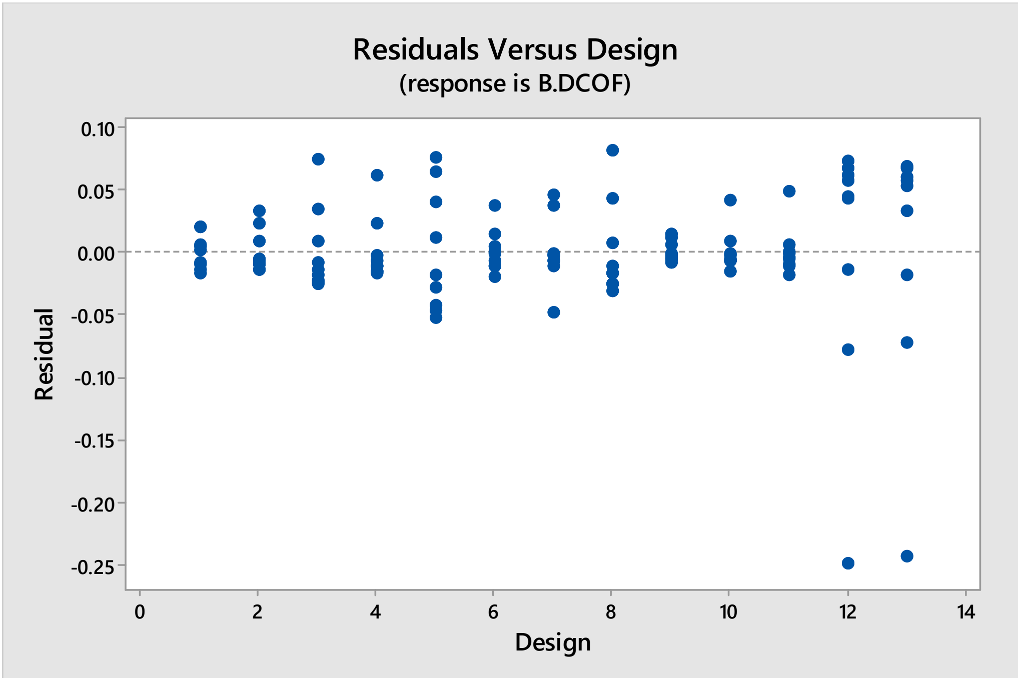

Figure 4-14: Residual plot versus design

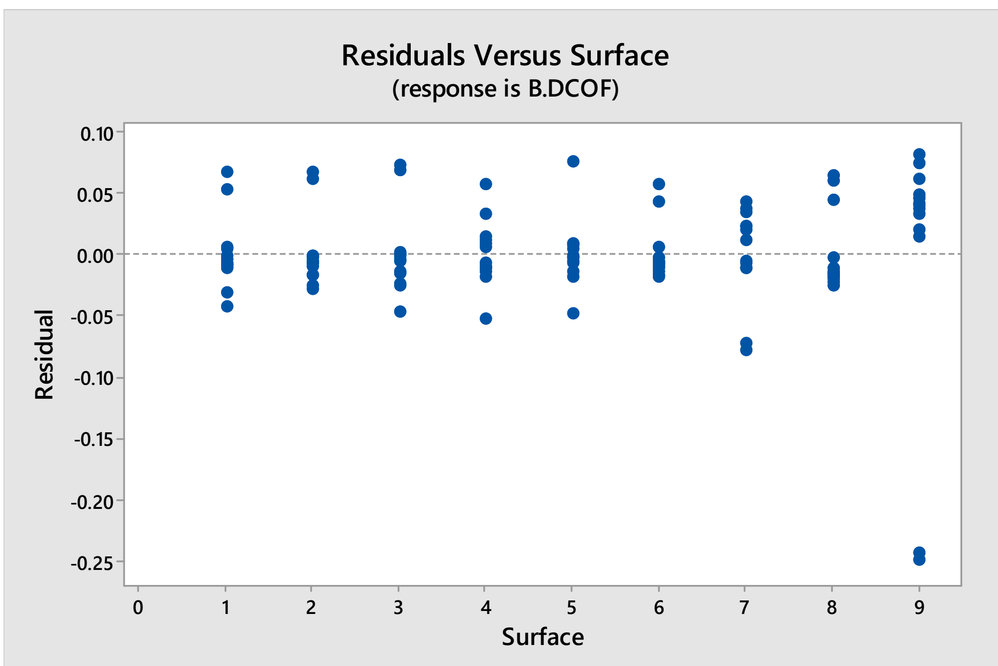

Figure 4-15: Residual plot versus surface

A Tukey comparison was done for the designs as well in order to see if there are any that appear to be statistically discernable from the rest but not from the barefoot testing. Means that share a letter are said to not be statistically discernable from one another, and values that do not share a letter are said to be statistically discernable from one another. Analysis shows that designs six and eleven are not statistically discernable from the values obtained via barefoot testing on the variable angle ramp. These designs will require additional research and broader range of surface testing in order to evaluate the relationship between the design and plantar skin. Analysis shows that other designs do not differ from one another. From the analysis utilizing the Tukey comparison it can be seen that two of the designs are grouped with the values obtained from barefoot testing. This means that statistically, the mean values of these factors are not discernable from one another. For the purpose of this thesis, this is an important finding that supports the data collected and shows that at least two of the designs, under the parameters listed for experimentation, performed close to the same as subject walking barefoot across the same surfaces.

Table 4-4: Tukey pairwise comparison

Tukey Pairwise Comparisons: Design

Grouping Information Using the Tukey Method and 95% Confidence

Design	N	Mean	Grouping				
5 – Parallel lines	9	0.280000	A				
1 – Concentric circles	9	0.241111	A	B			
8 – Perpendicular offset shark-skin	9	0.208889	A	B	C		
4 – Offset hexagons	9	0.198889		B	C	D	
2 – Justified cylinders	9	0.197778		B	C	D	
3 – Offset cylinders	9	0.196667		B	C	D	
10 – Perpendicular sine waves	9	0.188889		B	C	D	
9 – Parallel justified shark-skin	9	0.176667		B	C	D	
7 – Solid	9	0.154444			C	D	
11 – Parallel sine waves	9	0.132222			C	D	E
6 – Perpendicular lines	9	0.123333				D	E
12 – Test subject 1 barefoot data	9	0.060000					E
13 – Test subject 2 barefoot data	9	0.054444					E

Means that do not share a letter are significantly different.

A Tukey pairwise comparison graph was done for the samples that were grouped with the test subjects' barefoot values, this was done to graphically view the intervals. It is important to note that the parallel sine waves and perpendicular lines with the specifications mentioned in section 3.7.1 are not statistically discernable from the values obtained via variable angle ramp testing.

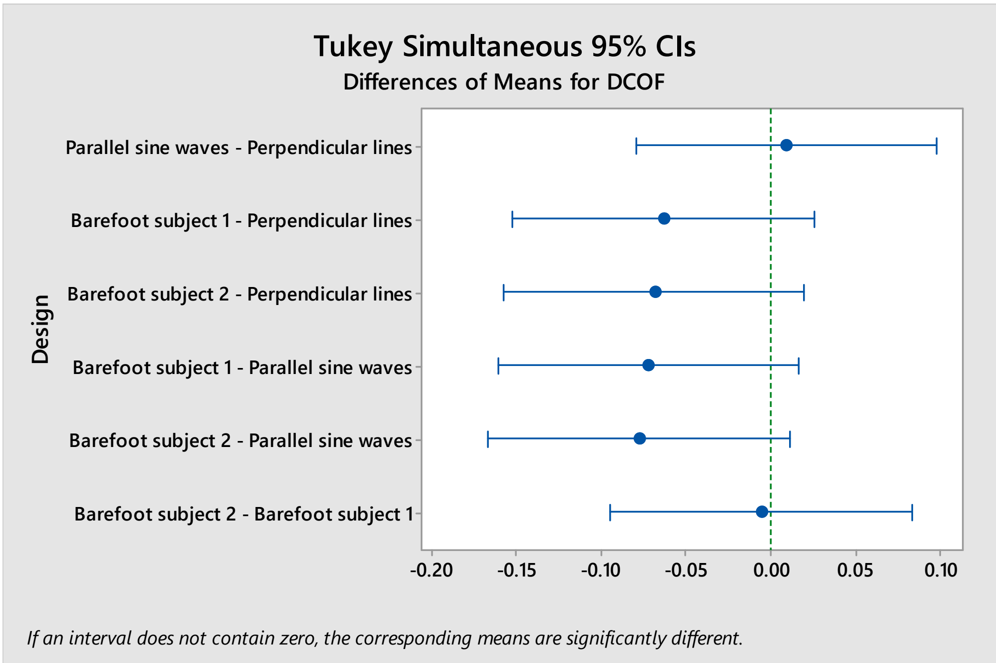

Figure 4-16: Tukey pairwise comparison of design six and seven to barefoot data

CHAPTER 5

CONCLUSION, RECOMMENDATIONS, AND FUTURE WORK

5.1 Concluding Remarks

The work presented in this thesis demonstrated successfully the potential of integrating biomimetic designs in replicating the frictional properties of human skin using additive manufacturing and walkway tribometers. Despite the primary focus of this thesis being on these applications, research into the effects commercially available treatments have on the measurable DCOF of surfaces was done as well. Treatment B showed promise in being able to consistently raise the DCOF of surfaces and additional research of this and similar products should be done on a broader range of surfaces. Now that a relationship between design, material, and plantar skin has been established research can be expanded into including treated/untreated surfaces and establishing a standardized limit of coefficient of friction on a surface in regards to walking barefoot. From the correlation table provided in section 2.1.5, the best correlation between the BOT3000E drag sled and the variable angle ramp is with the use of 10W-30 SAE oil. These findings are supported by comparing the biomimetic designs to subjects walking without footwear across the same surfaces under the same experimental conditions. A standardized limit would have a large impact on being able to properly assess the safety of a flooring surface and assist in litigation of insurance claims as well. This would also be able to increase the ability for companies to properly ensure due diligence in reducing the potential for STF accidents from occurring. The major highlights from this work are:

i. Analysis of commercially available treatments and the ability of these treatments to raise DCOF values. This can help to establish industry standards in application and treatment of surfaces deemed to be unsafe via ANSI A326.3.

ii. Setting up and proposing a methodology that can be adapted for development of biomimetic designs to be tested utilizing different equipment and different materials for designs.

iii. Study of direct light printing, materials, and limitations of these materials.

iv. Design, customization, optimization, and fabrication of biomimetic designs and their affect they have on measuring a wet DCOF value using 10W-30 SAE oil as a lubricant.

v. Achievement of similar values and statistical analysis showing designs grouped together with barefoot values via Tukeys pairwise comparison.

5.2 Recommendations of Future Work

The following recommendations when implemented will further improve the work presented in this thesis:

i. Design for AM by considering the guidelines and restrictions of AM throughout the proposal process.

ii. Consider the application of topology optimization on the selected designs for further mechanical behavior improvements.

iii. Apply designs into other systems and determine whether or not they impact the response variable and to what degree.

iv. Conduct fatigue and wear analysis of the printed designs to determine the capability to be produced on an industrial scale and a life cycle of the product.

v. Include more test subject varying in weight, height, ethnicity, and age to compare against designs.

vi. Include more surfaces for the designs to be tested on and increase the number of tests conducted on each surface to determine repeatability.

5.3 Conclusions and Further Design Improvements

It was found that two designs were grouped with barefoot testing data when using Tukeys pairwise comparison at a 95% confidence level. These designs are perpendicular lines (lines are perpendicular to the direction of travel of the walkway tribometer) and parallel sine waves (waves are parallel to the direction of travel of the walkway tribometer) In order to further improve the results obtained it is suggested that more testing be done with designs deemed similar to the values obtained from barefoot testing and expanding the surfaces to be tested on. Furthermore, in order to refine the results additional subjects varying in height, weight, age, gender, and ethnicity should be conducted to acquire a better representation of the human population for a better comparison. Another suggestion is to study the surface roughness and wettability of these surfaces and determine the relationship to the measurable DCOF. Changes should be made to the lubricant as well and determine the impact this has on the relationship between the designs and barefoot testing values. Additional designs can be tested and implemented along with repeating the testing with similar equipment to determine the ability to reproduce and replicate values obtained in this thesis. Expanding the designs into different materials and testing should be conducted as well. Finally research into a standardized limit of coefficient of friction for surfaces anticipated to be walked upon without proper footwear and wet should be conducted as well, similar to ANSI A326.3.

APPENDIX

TECHNICAL SPECIFICATIONS, TESTED SURFACES, AND DESIGNS

A.1 Technical Specifications

1. Soft polymer material properties:

Description	Value
Brookfield viscosity at 23°C	1.1 – 1.6 Pa's
Elongation at break	15-25%
Relative density	1.05 – 1.20 (water = 1)
Colors available	Pink

2. Ceramic-polymer material properties

Description	Value
Tensile Strength	39 MPa
Elongation at break	2.9%
Flexural strength	106 MPa
Flexural modulus	3760 MPa
Heat deflection temperature at 0.46 MPa	93°C

A.2 Tested Surface Images

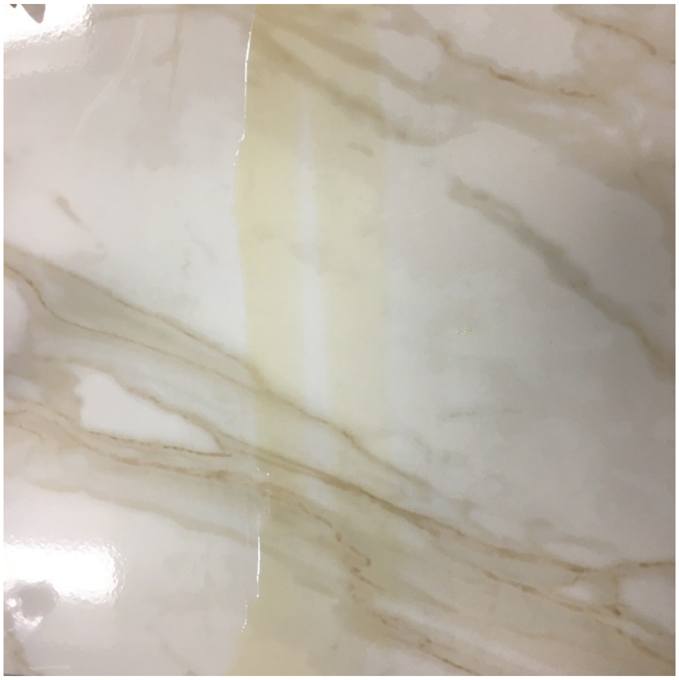

Figure A.1: Beige ceramic tile

Figure A.2: Polished black granite tile

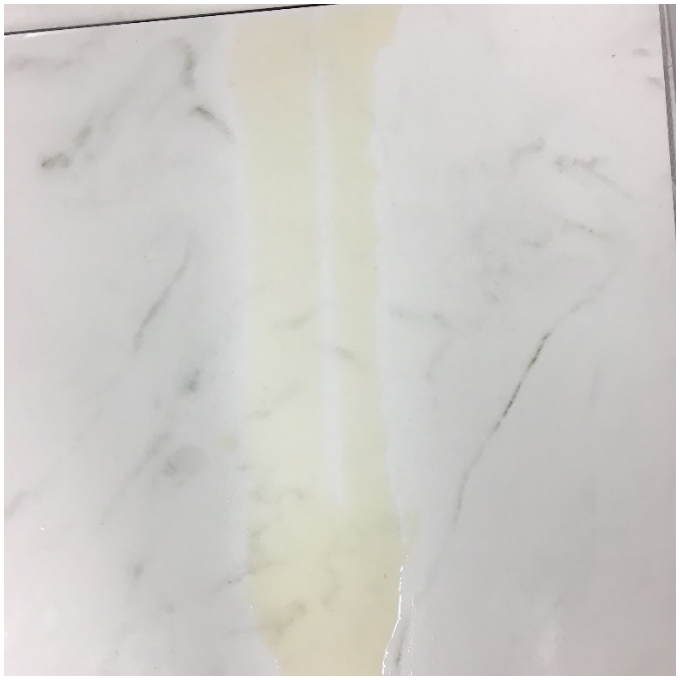

Figure A.3: White viena ceramic tile

Figure A.4: Polished white marble tile

Figure A.5: Travertine tile

Figure A.6: Polished porcelain tile

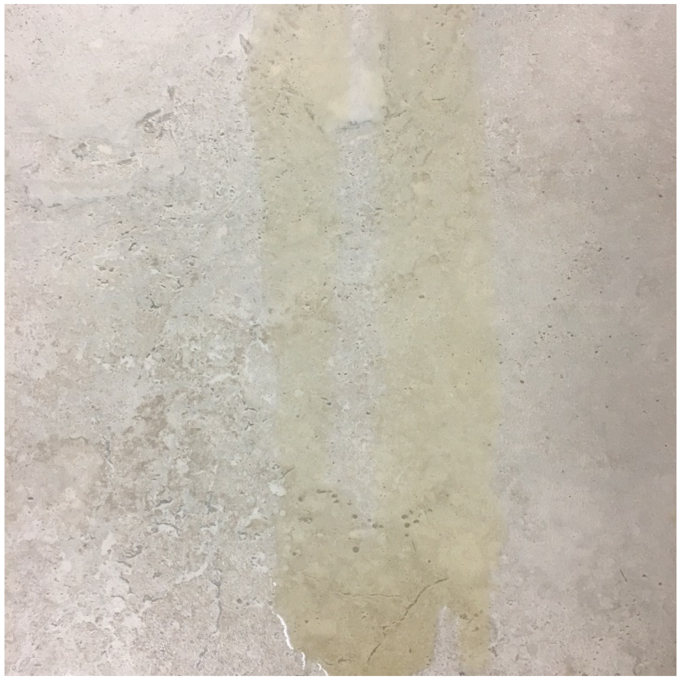

Figure A.7: Textured glazed porcelain tile

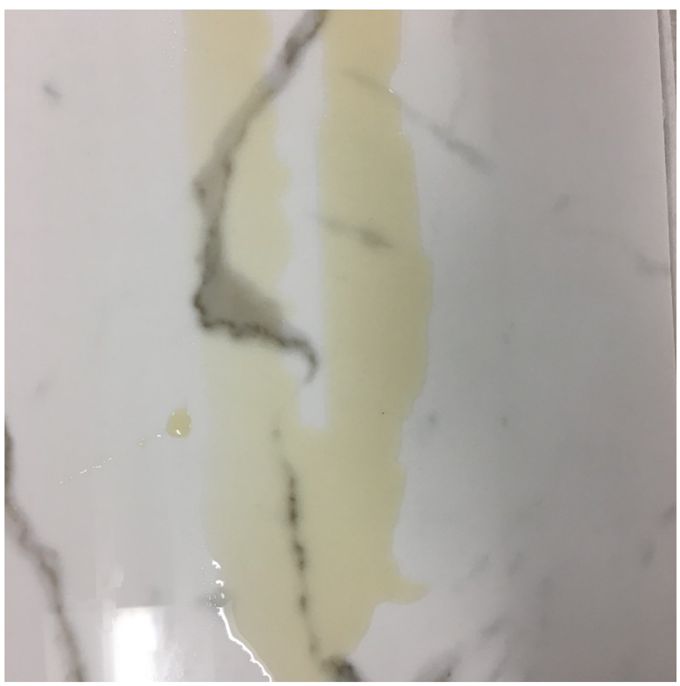

Figure A.8: Polished white porcelain tile

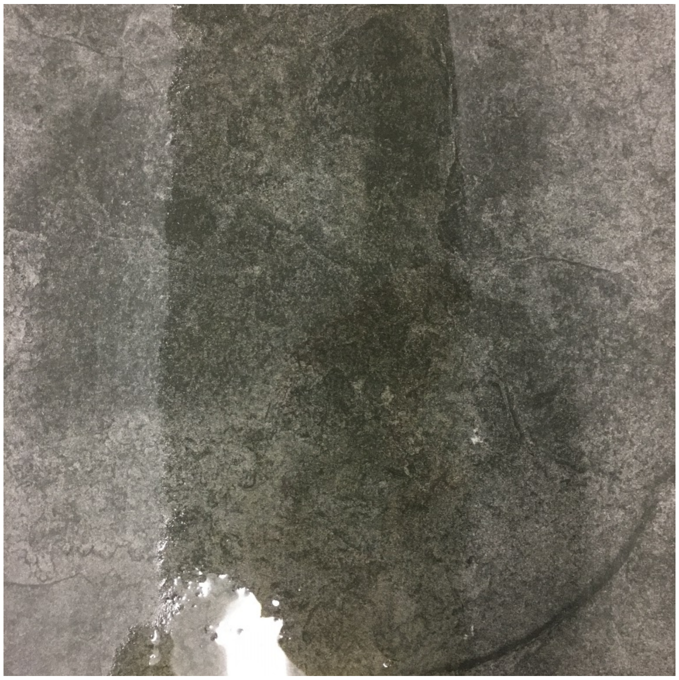

Figure A.9: Slate ceramic tile

A.3 Fabricated Designs

Figure A.10: Fabricated designs on sensor

COMPREHENSIVE REFERENCE LIST

[1] A. Tsipenyuk, M. Varenberg, Use of biomimetic hexagonal surface texture in friction against lubricated skin, J. R. Soc. Interface. 11 (2014).

[2] A.P. Malshe, S. Bapat, K.P. Rajurkar, H. Haitjema, Bio-inspired textures for functional applications, CIRP Ann. 67 (2018) 627–650.

[3] Q.W. Ri, English translation of DIN51130:2014-02, 6 (2014) 1–12.

[4] American National Standard Test Method for Measuring Dynamic Coe cient of Friction of Hard Surface Flooring Materials, 2018.

[5] S. Bönig, Experimental Investigation to Determine the Standardized Limit of the Coefficient of Friction for Slip Resistance During Walking, University of Wuppertal, 1996.

[6] D.I. James, The theory behind the DIN ramp tests, Polym. Test. 18 (1999) 3–10.

[7] K.A. Brown, K.R. Goodearl, K.A. Brown, K.R. Goodearl, Slip alert user guide, Lect. Algebr. Quantum Groups. 44 (2002) 281–288.

[8] H.T. Baker, A Study of Walkway Safety and Evaluation of Tribological Test Equipment, (2014).

[9] R. Grönqvist, M. Hirvonen, A. Tohv, Evaluation of three portable floor slipperiness testers, Int. J. Ind. Ergon. (2000).

[10] T. Council, N. America, A. American, N. Standard, S. Resistance, Excerpt ric Astrachan, Executive Director, Tile Council of North America. "Research E Supporting an ANSI American National Standard for Slip Resistance.," (2016) 2–9.

[11] J. Sebald, System oriented concept for testing and assessment of the slip ressitance of safety, protective and occupational footwear, Pro Business, 2009.

[12] E. Nr, Gleitfestigkeit in Barfussbereichen, (2004).

[13] M. Al-Assi, E. Kassem, Evaluation of Adhesion and Hysteresis Friction of Rubber–Pavement System, Appl. Sci. 7 (2017) 1029.

[14] V. Agostini, G. Balestra, M. Knaflitz, Segmentation and classification of gait cycles, IEEE Trans. Neural Syst. Rehabil. Eng. 22 (2014) 946–952.

[15] S.A. Arnadottir, V.S. Mercer, Effects of footwear on measurements of balance and gait in women between the ages of 65 and 93 years., Phys. Ther. 80 (2000) 17–27.

[16] M.M. Friedlander, Procedures for Evaluating Bathing Facility Slip and Fall Accidents by, (1976) 1–9.

[17] S. Derler, F. Kausch, R. Huber, Slip resistance in barefoot areas, (2004).

[18] F. Tiles, C. Lower, L. Upper, Barefoot Ramp Test DIN 51097 Shoe Shod Ramp Test DIN 51130 Pendulum Test BS7976-2, (n.d.) 24–26.

[19] EnvisionTEC, 3D-Printing-101-Stay-Flat-and-Parallel-03132017, (2017).